Aus dem Institut für Pathologie und Molekulare Diagnostik des
Universitätsklinikums Augsburg

Analysis of ctDNA in rectal cancer patients undergoing neoadjuvant radiochemotherapy (NeoRect trial)

Dissertation

zur Erlangung des akademischen Grades

Dr.rer.biol.hum.

eingereicht an der

Medizinischen Fakultät der Universität Augsburg

von

Tatiana Mögele

Augsburg, 16.05.2024

Universität
Augsburg
University

Eidesstattliche Versicherung und Erklärung

Hiermit versichere ich an Eides statt, dass die vorliegende Dissertation von mir selbständig und ohne unerlaubte Hilfe angefertigt wurde. Zudem wurden keine anderen als die angegebenen Quellen verwendet. Außerdem versichere ich, dass die Dissertation keiner anderen Prüfungskommission vorgelegt wurde und ich mich nicht anderweitig einer Doktorprüfung ohne Erfolg unterzogen habe.

Statutory declaration and statement

I declare that I have authored this thesis independently, that I have not used other than the declared sources/resources. As well I declare that I have not submitted a dissertation without success and not passed the oral exam. The present dissertation (neither the entire dissertation nor parts) has not been presented to another examination board.

Augsburg, 13.01.2025

Dissertation eingereicht am: 16.05.2024

Erstgutachter (Hauptbetreuerin/ Hauptbetreuer): Prof. Dr. Rainer Claus

Zweitgutachter: Prof. Dr. Pascal Johann

Tag der mündlichen Prüfung: 21.11.2024

Faber est suae quisque fortunae

Table of contents

1. Introduction

1.1. Rectal cancer

1.1.1. Pathogenesis and molecular model

In Germany, about one in eight cancers affects the colon or rectum in both sexes [1]. Rectal carcinomas (RC) are defined as tumors less than 17 cm away from the anocutaneus line. More proximal tumors until the ileocecal flap as colon carcinomas. Despite this anatomical definition, both have wide similarities in etiology and histology [2].

The risk of developing colorectal cancer (CRC) correlates positively with age and more than half of the cases are diagnosed in patients over 70 years with one third being located in the rectum [3]. After the introduction of precautionary coloscopies in 2002, the proportion of CRC diagnosed in late stadiums decreased resulting in a declined overall mortality rate (male: 29,6 to 19 per 100 000 and women 19 to 11,3 per 100 000 from 2000 to 2018) but still about 16.000 patients die from this malignancy yearly [4].

Besides age, some of the risk factors for CRC are diets rich in red and processed meat, low fiber intake, obesity and tobacco use. These factors can promote inflammation, oxidative stress, and metabolic dysfunction, thereby contributing to tumor initiation and growth. First-degree relatives of CRC patients have also higher risks of hereditary disease development even at younger ages than average [3]. Additionally to these environmental and hereditary factors, chronic inflammations in the colon like ulcerative colitis can further increase the risk of developing CRC [5].

As described by Eric R. Fearon and Bert Vogelstein in 1990, the pathogenesis of CRC is a complex and multifactorial process that involves a stepwise progression from normal cells to the formation of benign neoplasms (adenomas) and finally malignant tumors with an accumulation of genetic and epigenetic alterations [6]. About 70 to 90 percent of CRC arise from adenomatous polyps from single epithelial stem cells that have the potential to initiate the process of neoplasia by clonal expansion and to transform into malignant adenocarcinomas over time [5]. These adenomas gradually progress through increase in size and dysplasia and accumulate several genetic key lesions contributing to the process of tumorigenesis of CRC, such as genetic alterations in oncogenes and allelic losses among others. Genetic alterations like in the tumor suppressor gene *APC* (adenomatous polyposis coli) are associated to this classic adenoma-carcinoma sequence [7].

Another critical genetic event is the mutation of *RAS* genes. About 40% of CRC have found to harbor *RAS* gene mutations. Point mutations in this gene lead to somatic activation and increased levels of the coded protein which plays a key role in regulation of cell growth and differentiation. Its excessive accumulation results in uncontrolled cell mitosis and tumor expansion. In addition, this mutation leads to therapy options based on inhibition of epidermal growth factor receptors (EGFR) as often used for cancer treatment being in vain [8]. A variety of further mutations have been described in the context of CRC such as the tumor-suppressor genes *TP53*, *BRAF* and *PIK3CA*. Moreover, a subset of CRC cases exhibit microsatellite instability (MSI), a condition characterized by defects in the DNA mismatch repair system. This instability leads to a higher mutation rate, contributing to the development of CRC. Other molecular factors that can contribute to tumorigenesis are epigenetic modifications and chromosomal instability with loss of specific chromosomal regions [6].
In summary, RC develops through a complex interplay of genetic mutations, epigenetic changes, inflammation, and environmental factors. Early detection and screening play a crucial role in improving outcomes by identifying pre-cancerous lesions and early-stage cancers when treatment is more effective. Additionally, understanding the pathogenesis of RC can aid in the development of targeted therapies and molecular markers for disease monitoring.

1.1.2. Diagnosis and Screening

The long temporal progress from polyps to their malignant transformation gives the opportunity of early disease detection and prevention.
Precautionary coloscopies are generally considered the gold standard in RC screening with the main advantage of allowing diagnosis and definitive execution of polypectomy of adenomatous polyps and pre-cancerous neoplasms in early stadiums, therefore decreasing tumor-related mortality. According to German guidelines this screening method is recommended for men and women over 50 and 55 years, respectively, every ten years after inconspicuous results. On top of that, immunological faecal occult blood tests have a high sensitivity to detect hemoglobin which can be a first warning sign for RC and are therefore also recommended yearly from the age of 50 years [2]. To confirm the clinical or image-based suspected diagnosis, a rectoscopy is carried out to obtain material from suspicious lesions for histopathological assessment and molecular analysis, if applicable. After diagnosis, further analysis to exclude involvement of lymph

nodes and distant metastasis are conducted. This includes sonography and/or computer tomography (CT) or magnetic resonance imaging (MRI) of the abdomen. On top of that, carcinoembryonic antigen (CEA) levels are analyzed in blood during the course of disease [2].

Taking all results together, the identified tumor can be classified according to TNM (tumor, node, metastasis) criteria. This staging tool is the most useful and routinely used for surgical purposes. The TNM classification for RC is shown in Table 1.

Table 1: TNM classification for rectal cancer

Stadium	Primarius	Lymph nodes (ln)	Metastases
0	Tis	N0	M0
I	T1,T2	N0	M0
IIA	T3 T3a (<1 mm) T3b (1-5 mm) T3c (5-15 mm) T3d (>15 mm)	N0	M0
IIB	T4a	N0	M0
IIC	T4b	N0	M0
IIIA	T1-2	N1 (1-3 ln)	M0
IIIB	T3-4	N1 (1-3 ln)	M0
IIIC	all T	N2 (>3 ln)	M0
IV	all T	all N	M1

Modified from
https://www.onkopedia.com/de/onkopedia/guidelines/rektumkarzinom/@@guideline/html/index.html#ID0EJIAE, 06.03.2024, 09:08 a.m.

Tis: Carcinoma in situ (tumor cells only in mucosa)
T1: Tumor reaches submucosa
T2: Tumor reaches muscularis propria
T3: Tumor reaches subserosa or fat under muscularis propria
T4: Tumor additionally in other organs or peritoneum

N0: no lymph nodes included
N1: 1 -3 lymph nodes included
N2: over 4 lymph nodes included
M0: no metastases
M1: metastases

1.1.3. Treatment

The treatment plan for patients with RC is personalized based on staging (TNM classification), tumor characteristics and patient´s overall health. It typically involves a

multidisciplinary approach that combines surgery, chemotherapy, radiation and targeted therapies.

Surgery is the primary treatment option for localized RC with curative intention. Specially in early-stage cases, the goal is to remove the tumor and surrounding tissues to prevent spread of cancer. An adjuvant therapy regime using different chemotherapeutics to eliminate any remaining cancer cells can follow after resection depending on tumor stage and patient´s fitness [9].

In advanced stages of RC or cases with high risk of recurrence, the use of preoperative neoadjuvant therapy is indicated to shrink tumor size before surgery. In these cases of locally advanced RC, patients are first treated with neoadjuvant chemoradiotherapy (nCRT)- a combination of chemotherapy and radiation therapy to enhance the effectiveness. With the establishment of the surgical procedure of total mesorectal excision (TME), the risk of local recurrence in stage II and III is at 5 – 12%. Adding nCRT results in tumor downstaging and lowers therefore this number further [9-11]. Another treatment option for patients with certain high-risk tumor characteristics, e.g. N2- status, is the “total neoadjuvant therapy” (TNT) consisting of an additional chemotherapeutical treatment before or after nCRT. This strategy allows organ preservation in half of the patients with comparable disease-free survival (DFS) [12]. The optimal composition of TNT concerning the radiation regime for intended organ preservation is still focus of ongoing clinical studies [13].

Interestingly, in 20 to 30% of the cases treated with nCRT, a pathological complete remission (pCR) can be observed prior to TME. Subsequently, the benefit of the following surgical procedure is questionable as, besides the standard complications, there is a considerable risk of temporary or permanent problems with sexual function, bladder function and function of the anal sphincter [14].

A first clinical trial from Habr-Gama in 2004 showed 71 patients with an excellent outcome after clinical complete remission (CR) without TME. After a mean of 57 months an overall survival (OS) of 100% and DFS of 86% were reported [15]. Similar findings were observed in the OnCoRe project from 2016. Patients with clinical CR offered non-surgical management showed no difference in their 3-year non-growth DFS and OS compared with surgical resection but had significantly better 3-year colostomy-free survival [16]. In another study published in 2017 with a cohort of 370 participants, 69% of the patients showed a permanent CR. In 84% of the cases a local relapse was observed and treated successfully with a salvage-resection. When comparing the “watch and wait” (W&W) strategy and the group with the conventional TME after nCRT, both OS

and DFS were identical [14, 17]. Therefore, non-surgical treatment for locally advanced RC might constitute an oncologically safe treatment option for selected RC patients avoiding the morbidity associated with proctectomy. The prerequisites are an extensive interchange with the patient and the patient´s willingness to a more excessive aftercare with an active surveillance consisting of frequent follow-up including MRI and endoscopy [18, 19].

In this regard, the control group in the Habr-Gama study consisting of 22 patients with a chirurgical treatment after nCRT despite their clinical CR demonstrates the need of improvement in reliable (bio-)markers predicting pCR [15]. Accurate patient selection including precise classification of the residual tumor and strict selection criterias is crucial to identify cases eligible for an organ-preserving W&W approach [20, 21]. For instance, tumor regrowth has been shown to be associated to baseline T classification, as cT3 or cT4 patients with clinical CR are more likely to develop early tumor recurrence after a W&W approach [22]. It's been further reported that local regrowth appears in half of the patients classified to have a clinical CR within a year of follow-up. Here, organ preservation is still possible in over 78% of recurrences [23]. However, a study of 2019 reported worse survival in the W&W group with distant tumor progression in patients with local recurrence [20]. Further analyses of advanced RC in the International W&W Database (IWWD) confirm great long-term outcomes in patients with clinical CR after nCRT but report local regrow in 25,2%, 88% of which occurred within the first two years [24].

In addition, about 20% of the patients show no response to nCRT or progress under treatment. Even after evaluation of clinical tumor response with digital rectal examination, endoscopy and imaging together, a substantial portion of patients experience local regrowth with subsequent salvage treatments [25, 26].

Taken together, although a variety of methods have been discussed and were diagnostical significant in several studies none of them is suffice enough for the approach to predict tumor's response in the routine. This applies to imaging methods and laboratory, histologic and molecular markers [27-29]. Furthermore, overstaging of residual tumor still leads to a false diagnosis in 30 % of the patients with pCR highlighting the need of additional methods to provide a better picture of treatment response [30].

1.2. Liquid biopsy

1.2.1. Analytes in liquid biopsy

Liquid biopsy (LBx) is the umbrella term for the investigation of a variety of analytes from different body fluids. It was first described in 1869 and refers nowadays mainly to the analysis of genomic, proteomic and cellular/subcellular assessment of tumor-derived components in the context of cancer [31].
Most common body fluids that can be analyzed are blood, cerebrospinal fluid, pleural effusions and urin depending on target material and question of interest.

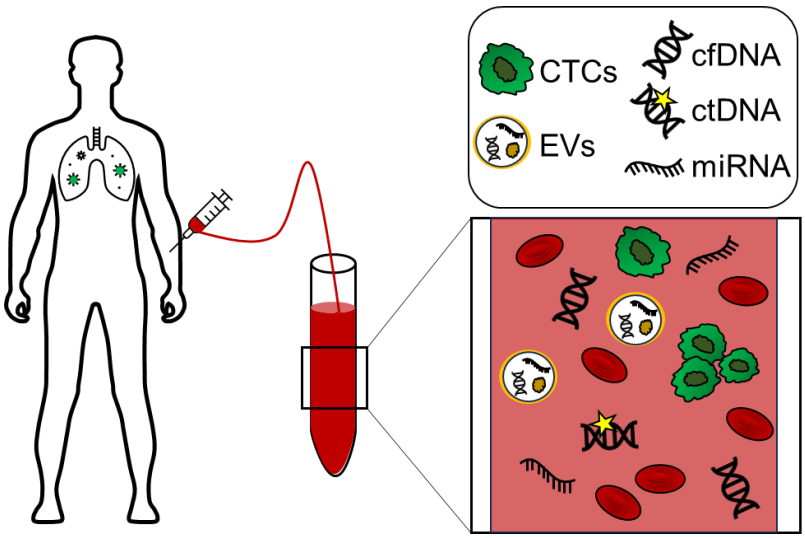

Figure 1: Schematic overview of the liquid biopsy composition in blood

These elements can be isolated from body fluids with different methods depending on the question addressed.
CfDNA: Cell-free DNA; CTCs: Circulating tumor cells; CtDNA: Cell-free tumor DNA; EVs: Extracellular vesicles; MiRNA: microRNA

The first LBx evaluation in peripheral blood of cancer patients was of circulating tumor cells (CTCs) [32]. Tumors shed cells with the potential to metastasize in distant body sites following the anatomical structures of the circulatory system. Measuring CTCs levels has gained immense significance. It has been reported to be a great indicator of treatment response and CTC´s dynamic to correlate with OS [33, 34]. Sophisticated methods have been established to enumerate CTCs within the heterogeneous cell population of the blood for routine diagnostics based on EpCAM (epithelial cell adhesion molecule)- positivity enabling a standardized examination of CTCs for breast, prostate and cancer patients providing a quick and easy way of tumor cell analysis without the

need of a tissue sample [35]. Furthermore, CTCs can be isolated and used for generation of patient-derived organoids as experimental models enabling further patient specific precision medicine [36].

Another candidate for LBx from biological fluids are extracellular vesicles (EVs). These exosomes are secernated from tumor cells and carry cell-specific endosomal and lysosomal biomolecules such as proteins, lipids and nucleic acids unmasking both genetic and proteomic information for potential therapeutic targets [37]. They have been described to promote tumor growth, immunosuppression and epithelial to mesenchymal transition (EMT) [38]. EVs are also involved in suppressing the tumor microenvironment and promoting a metastatic behavior of cancer cells [39]. Furthermore, EVs are known to be selectively taken up by other cells promoting cell-to-cell communication and reprogramming these, making them extremely interesting as therapeutic nanocarriers. Compared to CTCs, EVs can be found in cancer patients in high numbers. However, their heterogeneity poses major challenges in isolation efficiency and standardization limiting this technology for clinical applications [40].

Besides encapsulated in EVs, nucleic acids can also be found unbound in body fluids. Due to cell necrosis and apoptosis or active secretion, several types of deoxyribonucleic acid (DNA) and ribonucleic acid (RNA) molecules are released. Within the group of RNAs, both coding and non-coding RNA (ncRNA) are present [41]. Yet, ncRNA tend to form secondary structures and are more often associated with proteins resulting in a higher stability than protein coding single strand mRNAs and are therefore better studied. NcRNAs have a wide variety of functions within cells: They are involved in the process of translation (tRNA, rRNA) and have effects on posttranscriptional gene regulation (e.g. miRNA, siRNA) among others. It has been shown that expression levels of ncRNAs detected in blood differ between healthy individuals and cancer patients offering a suitable biomarker candidate for diagnostic and prognostic tests [42, 43].

Besides RNA, cell-free DNA (cfDNA) can be also detected. The significance of this material for different diseases was already described by Tan and colleagues in 1966 in the context of patients with systemic lupus erythematosus [44]. Following these findings, many studies have focused on cfDNA levels in blood within different patient groups. It has been shown to be a prognostic marker for myocardial infarction and a predictor for severe sepsis and septic shock besides many other potential uses in e.g. the context of cancer [45, 46]. On top of that, the discovery of circulating fetal DNA in plasma of pregnant women in 1997 lay the foundation for non-invasive prenatal genetic diagnostics (non-invasive prenatal testing, NIPT) [47]. This method is used for detection of common

fetal genetic anomalies such as chromosomal disorders, specially trisomies, but also subchromosomal aberrations and monogenic disorders in early pregnancy status [48]. It has been implemented into routine diagnostics due to its non-invasiveness, especially for the fetus, but high accuracy in detection. This example highlights the potential of LBx for a variety of clinical inquiries.

Taken together, minimal invasive character of LBx enables repeated sampling for continuous disease monitoring increasing the chance for early tumor evolution description and drug response mechanisms. Furthermore, it gives spatial and temporal information about tumor heterogeneity without the need of histological evaluation resulting in shorter time and lower costs of sample isolation. On top of that, a wide variety of aspects can be examined from LBx – whole tumor cells, proteome, metabolite and transcriptome profiling and different genomic aspects such as copy number variations, mutations and epigenetic alterations [32].

Despite much clinical evidence implicating the role of LBx, the method has been shown to be insufficiently able to substitute its tissue counterpart and most of the analysis are still to be validated in clinical practice [49]. Therefore, tissue genotyping remains the gold standard in cancer diagnosis for identification of genomic alterations despite several limitations of this technique.

1.2.2. Characteristics of circulating DNA and methods of detection

As described above, cfDNA can be detected in plasma. It originates from cell death like necrosis and apoptosis, specially of lymphoid and myeloid cells, so as low levels are physiologically measured in every individual independent of any disease.

CfDNA is assembled like genomic DNA with the classic double-helix shape. However, compared to high molecular genomic DNA, cfDNA is highly fragmented into short sequences of about 180 basepairs (bp) corresponding to nucleosome-associated DNA [50].

As first described by Leon and colleagues in 1977 in oncological patients a proportion of cfDNA is released from tumor cells [51]. The ratio of this specific cfDNA, the so-called circulating tumor DNA (ctDNA) can vary greatly ranging from 0,1-90% depending on several aspects such as tumor type, tumor burden, therapy regime, among others [52].

Once these molecules are released into the bloodstream, cfDNA is exposed to both, physiological processes of DNA degradation and immunological reactions such as digestion through macrophages. Consequently, cfDNA has a relatively short lifetime

within the systemic circulation of around 2 hours. On top of that, after blood draw, rapid sample processing is required, as other cellular components start degrading and lead to dilution of ctDNA of interest through release of gDNA. Taken together, ctDNA studies require sophisticated technologies with low limits of detection (LoD) equivalent to 0,1% variant allele frequency (VAF) or below [53, 54].

Various methods have been developed to detect and analyze ctDNA, offering a range of sensitivities, specificities and applicability to different cancer types. (Figure 2)

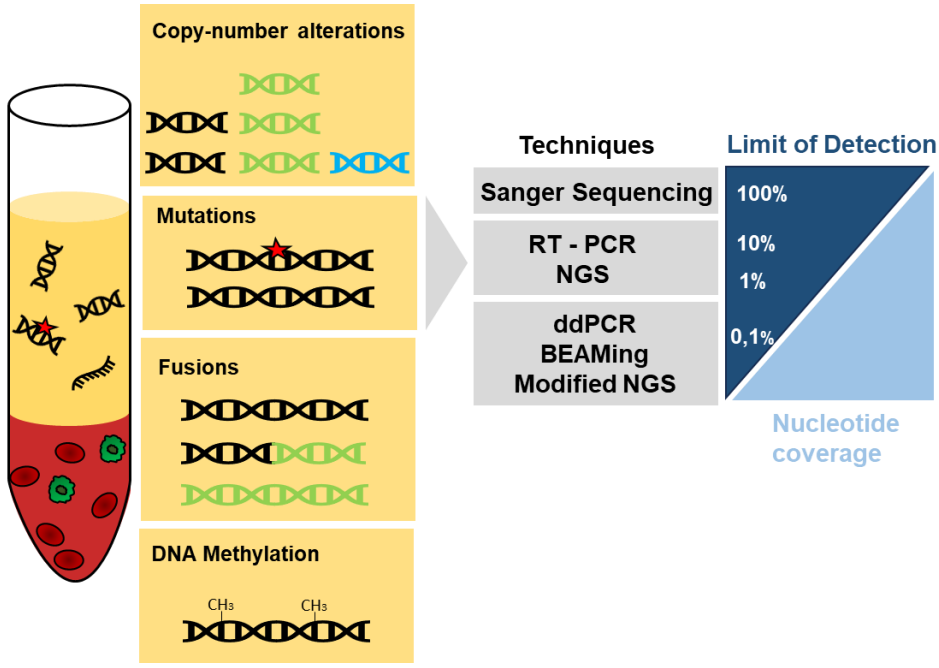

Figure 2: Overview of common DNA-based alterations that can be identified in plasma and specialized methods for ctDNA analysis according to their nucleotide coverage and limit of detection

BEAMing: Beads, Emulsion, Amplification and Magnetics; ddPCR: digital droplet polymerase chain reaction; NGS: Next Generation Sequencing; RT-PCR: Real time- polymerase chain reaction

The initial techniques for ctDNA analysis were based on polymerase-chain-reaction (PCR). However, the very low number of tumor related alleles makes detection challenging. A general approach to tackle this matter was introduced by Sykes and colleagues in 1992. Digital PCR (dPCR) is a method of absolute nucleic acid quantification by partitioning the sample for amplification into many individual microreactions allowing a sensitive and quantitative detection of rare mutations present in cfDNA. Identification of mutated DNA molecules can be then assessed by counting fluorescently labeled probes. This is the basic mechanism for a variety of ultrasensitive

methods such as BEAMing (beads, emulsion, amplification and magnetics) and droplet digital PCR (ddPCR) [55].

The BEAMing technology combines emulsion PCR and dPCR. Herein, wildtype DNA (wtDNA) and mutated DNA bind to streptavidin-coated magnetic beads with specific primers and are amplified by PCR in emulsion. Consequently, thousands of copies of the original molecules can be isolated from emulsion and purified with a magnet. After denaturation and fluorescent staining the number of variant DNA molecules in the population can be assessed using flow cytometry [56]. Similarly, ddPCR portions the sample into thousands of oil droplets with all reagents needed for amplification without the need of magnetic beads. After PCR, the droplets are also read by fluorescence enabling absolute quantification of ctDNA mutations. It is a highly reproducible and precise method suitable for detecting low-frequency variants [57, 58]. Altogether, these PCR-based methods can identify and quantify individual point mutations in a high sensitive manner with an allele frequency of 0.1% in cfDNA.

In contrast to the analysis of single loci via dPCR, next generation sequencing (NGS) is a massively parallel sequencing technology that enables simultaneous analysis of multiple genetic alterations in cfDNA. It can be designed to target single regions of interest, the whole exome or genome. But there are limitations to this technique as it accumulates errors resulting in the generation of false positive results**.** Sources can be potential sequencing errors or polymerase errors in specific regions. Therefore, refinement strategies have been developed for error reduction. One of these is the usage of molecular barcodes (unique molecular identifiers (UMI)) to enable discrimination of true mutations present in cfDNA from those potentially introduced by polymerases during sequencing reaction. This together with other modifications enable LoDs of 0,1%.

Furthermore, hybrid capture-based approaches for specific mutations followed by NGS for mutation profiling can offer a balance between sensitivity and cost-effectiveness [54]. Taken together, these technologies enable highly sensitive ctDNA detection making it a useful tool for different applications in the context of cancer.

1.2.3. Applicability of ctDNA in the context of cancer

One potential application of LBx is the early cancer detection in an otherwise asymptomatic population. Patients with early-stage cancers show specific alterations in driver genes related to solid tumors and their ctDNA depict high concordance with tumors´ alterations [59]. Nonetheless, de novo identification of somatic mutatios for early cancer detection remains a major challenge due to several limitations including the need

for high sensitivity, specificity and massive parallel analysis of potential driver genes, identification of tumorous tissue (as many cancer types share common mutations) and minimization of false positive results caused by genetic alterations related to clonal hematopoiesis. However, next to the image-based standard procedures for tumor diagnosis, tumor molecular profiling has become crucial for the selection of therapy in cancer patients. As described above, ctDNA detection from peripheral blood draw has the potential to assess tumor´s molecular profile without the need for an invasive biopsy [53, 60]. Therefore, once a tumor is identified, LBx is a powerful tool for tracking of crucial mutations such as *KRAS* mutations in patients with RC before applying targeted therapy. Thierry and colleagues compared *KRAS* mutation status from gold-standard tissue biopsy with corresponding cfDNA. For seven different *KRAS* point mutations they showed a concordance value of 96%. This result emphasizes the power of this procedure and its potential to question the need of invasive tumor biopsies for genetic analysis in a clinical context [61].

Furthermore, the non-invasive manner of LBx is a key feature that enables multiple sampling for longitudinal monitoring and therefore tracking of therapeutic response. Several groups have analyzed this aspect in different settings [62]. For instance, ctDNA levels measured sequentially during neoadjuvant therapy of breast cancer patients appear to be predictive of local tumor response and patient recurrence after therapy completion even outperforming imaging in predicting the overall response [63, 64]. Another study categorizes patients with non-small-cell lung cancer (NSCLC) into three groups according to the course of serial assessment of *EGFR* mutations in cfDNA - fast clearing of ctDNA as a sign for therapy response, no detection being correlated with stable disease and dramatic increase of ctDNA levels in plasma correlated with tumor progression and therefore poor patients´ survival [65].

Similarly**,** the possibility to monitor longitudinally during treatment and the advantage of depicting intra and inter tumoral genetic heterogeneity enable monitoring for resistance mechanisms arising during therapy. The T790M mutation of the *EGFR* gene in NSCLC is a classic example of a resistance mechanism that progresses under treatment. It is crucial to switch to a subsequent therapy after its detection. Sequential liquid biopsies can determine T790M mutation status and therefore influence patients´ therapy and lead therefore to a more successful treatment without the need for repetitive invasive methods [66].

Lastly, measurements of ctDNA after surgery offer a highly sensitive method for detection of minimal residual disease (MRD) and recurrence risk. In patients with stage II colon

cancer, it was shown that LBx can identify individuals with high risk of recurrence even superior to clinicopathological measures currently used highlighting its potential as a therapy guiding biomarker [67].

1.3. The NeoRect trial

The focus of this thesis is to monitor RC patients in the context of nCRT in the NeoRect trial using LBx. The aim of this study is to enroll patients with locally advanced RC who are eligible for nCRT and undergo standardized clinical management with additional systematic LBx. In this context, we will explore the quantity of cfDNA during nCRT, the detection of informative mutations in ctDNA before and its dynamics during therapy and correlate these results with imaging according standard of care, tumor markers and histological remission status after surgery.
We hypothesize that a multimodal assessment including these parameters and LBx will allow prediction of clinical and histopathological response after nCRT and therefor have the potential to impact the decision towards a W&W approach in the long-term to develop and validate a robust approach for detection of ctDNA using dPCR.

1.3.1. Methological validation as foundation for ctDNA analysis in the clinic

A preliminary sub aim is to establish a protocol for detection of ctDNA applicable for different approaches in the context of cancer in the University hospital of Augsburg. For analytical validation of this quantitative test, sensitivity, specificity, LoD and reproducibility will be evaluated. Further parameters such as applicability and feasibility will be taken into consideration to lay the foundation for a standardized protocol in the clinic.

.

2. Materials und Methods

2.1. Materials

2.1.1. Kits

Table 2: List of used kits

Kit name	Supplier
Agilent High Sensitivity DNA Kit	Agilent Technologies
Maxwell ® ccfDNA Plasma Kit (AS1480)	Promega
Maxwell ® 16 FFPE Plus LEV DNA Purification Kit (AS1135)	Promega
Maxwell ® RSC LV ccfDNA Kit (custom AX1115)	Promega
QIAamp MinElute ccfDNA Midi Kit	Qiagen

2.1.2. dPCR assays

Table 3: List of dPCR assays from Applied Biosystems

dPCR assay ID	Gene	Hotspot
BRAF_476	*BRAF*	V600E
EGFR_6240	*EGFR*	T790M
KRAS_19404	*KRAS*	A146T
KRAS_19900	*KRAS*	A146V
KRAS_516	*KRAS*	G12C
KRAS_517	*KRAS*	G12S
KRAS_518	*KRAS*	G12R
KRAS_520	*KRAS*	G12V
KRAS_521	*KRAS*	G12D
KRAS_532	*KRAS*	G13D
NRAS_584	*NRAS*	Q61R
PIK3CA_763	*PIK3CA*	E545K

PIK3CA_775	*PIK3CA*	H1047R
TP53_10662	*TP53*	R248Q
TP53_10704	*TP53*	R282W

2.1.3. Other chemicals

Table 4: List of other reagents

Reagent	Supplier
AmpliSeqCancer HotSpot Panel	Illumina®
AmpliSeq™ CD Indexes	Illumina®
AmpliSeq™ Library PLUS	Illumina®
GAPDH157	Applied Biosystems
Nuclease-free water	Thermo Scientific
QuantiFluor ONE dsDNA Dye	Promega
QuantStudio™ 3D Digital PCR Master Mix v2	Applied Biosystems
T790M mutated genomic DNA	Horizon Discovery
TaqMan ® Fast Advanced Master Mix	Applied Biosystems

2.1.4. Equipment

Table 5: List of equipment

Equipment	Manufacturer
Agilent 2100 Bioanalyzer instrument	Agilent Technologies
Centrifuge 5425	Eppendorf
Centrifuge Rotina 420R	Hettich Zentrifugen
Chip Priming Station	Agilent Technologies
IKA® MS 3 Vortexer	Agilent Technologies
Illumina MiSeq	Illumina®
LightCycler 2.0	Roche
Mastercycler X50I, PCR Cycler	Eppendorf

Maxwell CSC	Promega
miniFuge Centrifuge	Fisherbrand
ProFlex™ PCR System Dual Flat Block Thermal Cycler	Applied Biosystems
QuantStudio 3D ChipReader	Applied Biosystems
QuantStudio 3D Digital PCR Chip Loader	Applied Biosystems
QuantStudio 3D Digital PCR System	Applied Biosystems
Quantus™ Fluorometer	Promega
ThermoMixerC	Eppendorf
VacConnector on the QIAvac 24 Plus	Qiagen
Vortex-T Genie ® 2	Scientific Industries

2.1.5. Consumables

Table 6: List of consumables

Consumables	Supplier
EDTA-tubes Monovette®	Sarstedt
15 ml falcon tubes	Sarstedt
High Sensitivity DNA Chip	Agilent Technologies
QuantStudio™ 3D Digital PCR 20K Chip	Applied Biosystems
V2 flowcell MS-102-2002	Illumina®
DNA LoBind Tubes 1.5 ml	Eppendorf

2.2. Trial design and patient inclusion

We performed a retrospective noninvasive ctDNA study on prospectively collected samples from early RC patients enrolled in the single center neoadjuvant NeoRect trial between December 2017 and September 2019. Patients with stage II/III RC were eligible. All patients signed informed consent. Patients were screened for metastatic disease by imaging prior to enrollment, and those with de novo metastatic disease were excluded.

Diagnosis and nCRT were performed according to standardized procedures in accordance with current guidelines. Initial diagnostics included rigid rectoscopy to determine the exact height of the carcinoma, obtaining deep biopsies for histopathological and molecular analysis, assessing local tumor topology by MRI, and staging by CT thorax/abdomen exclusively in the context of established routine

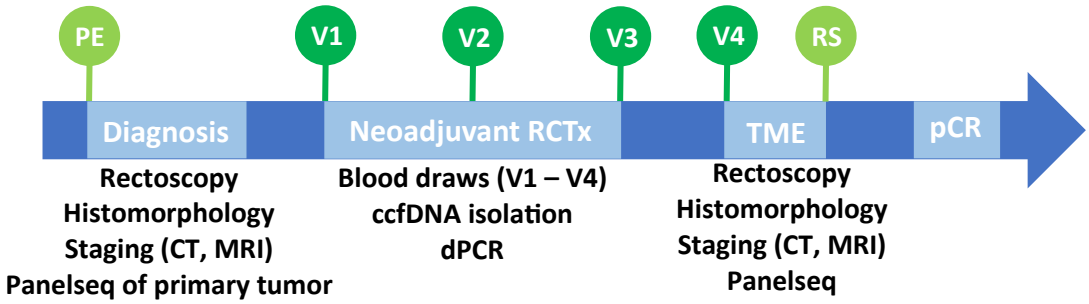

Figure 3: Overview of the NeoRect trial

At the time of diagnosis, the tumor is assessed in the context of routine diagnostics by rectoscopy and MRI. A tissue sample is also obtained for histomorphological classification and molecular analysis. During neoadjuvant treatment (nCRT) until surgery (TME) four blood draws (V1 – V4) will be conducted for cfDNA isolation and ctDNA analysis by dPCR. A second rectoscopy and staging will be conducted in the context of surgery and histopathological remission status will be defined by the pathologists.
ccfDNA: circulating cell-free DNA; dPCR: digital PCR; RCTx: Radiochemotherapy; RS: remission status; pCR: pathological complete remission; PE: pathological exision

diagnostic procedures. Neoadjuvant therapy was performed by the local oncology clinic in a standardized manner according to the "Sauer" protocol (Figure 4).

The required examinations for remission assessment before resection were part of the standardized procedure according to the guidelines and were analyzed regarding tumor stage, mesorectal fascia infiltration, tumor volume, MRI-based tumor regression grade and lymph node status. CEA was measured as part of routine clinical diagnostics and therapy monitoring.

After successful neoadjuvant therapy and TME, a detailed histological examination of the surgical specimen was performed with collection of all standard parameters. The tumor area was completely transversely lamellated, precisely photo-documented and processed in large-area sections.

To identify informative biomarkers for ctDNA analysis, multiple deep biopsies were obtained with a total volume of at least 1 cm^3 and analyzed by targeted panel sequencing as described below.

Peripheral venous blood was obtained from the respective study participant (4 x 9 ml in EDTA) at four time points – Visit 1 (V1) after diagnosis and before start of nCRT, Visit 2

(V2) during and Visit 3 (V3) after nCRT and Visit 4 (V4) before TME. All samples ran through the protocol established for LBx analysis beforehand.

2.3. „Ethik- und Tierversuchsvotum“

For the conduct of the trial, a consultation and a vote of the Ethics Committee of the Ludwig-Maximilian-University Munich were obtained (Project number: 17-586). The documents for informing the study participants and the forms for written consent were enclosed with the ethics application. The ethical principles are outlined in the Declaration of Helsinki ICH GCP. All usual precautions for data protection were taken.

2.4. NGS panel sequencing of tissue biopsies for identification of informative mutations

To confirm the diagnosis of RC histologically, biopsies of the primary tumor were formalin-fixed and paraffin-embedded (FFPE). A 2 µM-thick section was obtained from the FFPE tissue and then stained with hematoxylin and eosin for pathologic evaluation. For molecular analysis, tumor cells were acquired using microdissection under histomorphological control. The percentage of tumor cells in the microdissected areas was documented. Genomic DNA was isolated with a Maxwell ® 16 FFPE Plus LEV DNA Purification Kit (Promega, AS1135) and fluorometrically quantified with Quantus (Promega). For long-time storage DNA was stored at -20° C.

DNA panel sequencing addressing hotspot regions of 50 genes with known associations to cancer was performed for molecular analysis of activating mutations and in the context of the standard management and in order to identify a clonal biomarker for plasma monitoring. The library was prepared using AmpliSeq™ Library PLUS for Illumina®, AmpliSeqCancer HotSpot Panel for Illumina® and AmpliSeq™ CD Indexes for Illumina® according to the supplier’s manual. The DNA-input varied between 1 and 100 ng DNA/sample. The final libraries were fluorometrically quantified with Quantus (Promega), pooled, diluted to a final concentration of 8 pM and sequenced on the Illumina MiSeq using paired 150 bp reads on a V2 flowcell (Illumina, MS-102-2002). Sequencing was conducted with a mean coverage of ≥1000 reads. BCL files were converted to FASTQ and VCF files using the DNA amplicon workflow application on the LRM software from Illumina. BaseSpace Variant Interpreter from Illumina was used for variant calling. Results were filtered for nonsynonymus substitutions and non-polymorphic changes. Only point mutations (no deletions or insertions) with frequencies over 5% were taken

into consideration. Detected mutations with respective VAFs were documented on Microsoft Excel.

2.5. Clinical assessment

A variety of clinical parameters was assessed for evaluation of response to nCRT in the context of routine diagnostics before TME.

2.5.1 Radiography

Radiographic assessment and response evaluation were conducted by experienced colleagues of the department of radiology at the clinics of Augsburg.
Pelvic MRIs were performed at 1,5 T before and after neoadjuvant treatment using 2D T2 weighted sequences in 3 planes and axial DWI Sequences (highest b-value B 900) with calculated ADC maps as a standard protocol. Tumor visualization was improved by application of rectal gel and intravenous administration of a spasmolytic agent (butylscopolamine).
MR-morphologic response to neoadjuvant treatment was graduated from score 0 to score 4 according to 5 patterns, depending on the quantity of change in tumor volume and / or tumor signal. Change of tumor tissue to fibrosis was defined by absence of restricted diffusion (characterized by high DWI signal with corresponding low signal in ADC-maps) with hypo- to isointense signal in T2, whereas changes of tumor tissue to granulation tissue was defined by absence of restricted diffusion with persisting hyperintense signal in T2.
CT scans were performed before starting radiation without intravenous contrast media according to routine standards. Images were obtained with patients in prone position from the third lumbar vertebra to the caudal edge of the trochanter minor femoris. Afterwards, 5mm scans were reconstructed to find a point of reference for radiation. After nCRT and before surgery, CT scans were conducted for restaging according to local standards using intravenous contrast media unless contraindicated.
Complete response to nCRT was defined by either no visible residual tumor or complete fibrosis / granulation of residual tumor volume. Partial response included subgroups of good, moderate and poor response, depending on the proportional reduction in tumor size to baseline and / or proportional transformation of residual tumor volume to fibrosis / granulation. Progressive disease was defined by tumor growth with persistent tumorous signal and stable disease by no changes in tumor signal or volume.

2.5.2 Rectoscopy

Evaluation of rectoscopies´ results was conducted by experienced colleagues of the surgical department of the University hospital of Augsburg. Rectoscopies were performed in the context of routine diagnostics before neoadjuvant therapy and before TME. Tumors´ locations were described by their lower tumor edge in cm ab ano. Rectoscopic response was reported based on differences observed between pre-therapeutical and pre-surgical evaluation regarding size, scarring and observation of surrounding tissue, mucous membrane and lymph nodes among others. Patients with at least one external staging were classified as not assessable. All other individuals were categorized as good, moderate or no response. The definition of “good response” is therefore an overall improved perception but not necessarily equivalent to no residual tumor.

2.5.3 Carcino-embryonic antigen

The carcino-embryonic antigen (CEA) is a glycoprotein measured in patients with RC as a control during therapy, for identification of residues after surgery and as assistance for tumor classification. The values within a patient sample can vary depending on the procedure used. Here, CEA was measured at the institute of laboratory medicine and microbiology in the context of routine diagnostics using the ElectroChemiLuminescence-ImmunoAssay “ECLIA” for immunological in-vitro quantitative determination from plasma samples. The analyses were conducted on the cobas 8000 e801 immunoassay system based on standard curves generated from samples included in the reagent kit. Resulting concentrations were recorded as ng/ml (1 ng/ml CEA = 16.9 mIU/ml).
Plasma samples evaluated in this trial were collected before surgery from the same blood draw as for LBx analysis.
Values between 0 – 3,8 ng/ml were defined as physiological according to the local standard. Values higher than 3,8 ng/ml were not further quantified but remarked as generally elevated.

2.5.4 Pathology

In the context of routine diagnostics, patients´ biopsies were evaluated by experienced pathologists of the department for pathology and molecular diagnostics and described based on the TNM classification for RC if applicable [13]. Grading (G) defined as the tumor´s nature in terms of histopathological differences between normal and tumor tissue

was documented. The higher the G value (G1 – G4), the less differentiated appear tumoral cells and therefore the more aggressive the tumor.
After treatment, if surgery was conducted at the University hospital of Augsburg, pathologists of this department described the surgical specimens for response evaluation. According to the assessed pathological features of the primary tumor after TME, the specimen is classified into a five-tier grading system initially described by Dworak in 1996 [68]. This scoring describes the range of pathological response, with a Dworak value of 0 meaning no regression and the highest value of 4 being a total regression or complete pathological response (pCR) after therapy.
Taken all the evaluations together, individuals were characterized as showing a pCR, a subtotal remission (SR), or no pCR.
Pathological assessment (specially Dworak scoring and response evaluation) of the specimen after surgery was defined as the groundtruth concerning the response to overall treatment and used for correlation analysis with other modalities and LBx within this trial.

2.6. Liquid Biopsy

2.6.1. Plasma and cfDNA isolation

Whole blood was collected in 9 ml EDTA-tubes (Sarstedt Monovette®). Plasma and cells were separated within three hours after blood draw to avoid contamination from lysed lymphoid and myeloid cells. Therefore, first, the EDTA-tubes were centrifuged at room temperature (RT) at 2000 xg for 10 minutes and stopped at low-speed. From each tube, four times 1,1 ml plasma were aliquoted into sterile 1,5 ml tubes. After a second centrifugation step at RT and 15.000 xg for 10 min, 1 ml of each supernatant was transferred into fresh 1,5 ml tubes. For long-time storage, the aliquots were kept at -80°C. Until further usage and ccfDNA isolation, plasma was stored at -20° C.

Promega isolation method

The first method used for cfDNA isolation was with the Maxwell ® RSC LV ccfDNA Kit (Promega, custom AX1115). One to four millilitre plasma were mixed with equal amounts of binding buffer and 140 µl magnetic resin in 15 ml falcon tubes (Sarstedt) and incubated in a rotisserie shaker for 45 min at RT. This leads to random ligation of magnets to the cfDNA. Thereafter, the suspension was centrifuged for 2 min at 2000 × g to pellet the magnetic beads ligated to the cfDNA. With the help of a magnetic stand to prevent losing

material, the supernatant was carefully decanted and the magnetic pellet harboring the DNA was resuspended with buffer. The final mixture was transferred into the Maxwell catridge provided by the kit. After automated isolation in the Maxwell instrument (Maxwell CSC, Promega) the final cfDNA was eluted in 60 µl elution buffer included in the kit and stored for long-term at -20 °C.

Qiagen isolation method

The second method applied for cfDNA isolation was using the QIAamp MinElute ccfDNA Midi Kit (Qiagen). All reagents and buffers are provided by the kit. As with the Promega protocol, an input amount of 1 - 4 ml plasma was combined with 100 µl proteinase K and 800 µl ACL buffer per milliliter sample. After incubation at 60 °C for 30 minutes (ThermoMixerC, Eppendorf), 1,8 ml ACB buffer per milliliter sample were added and further incubated for 5 min on ice. The lysate-buffer mixture was applied into a 20 ml tube extender placed into an open QIAamp Mini column connected to a vacuum pump (VacConnector on the QIAvac 24 Plus, Qiagen). The vacuum pump helps pulling the high volume of liquid through the membrane rapidly while DNA molecules get attached to the membrane. To wash the membrane and therefore the DNA, 600 µl and two times 750 µl ACW1, ACW2 buffer and 100 % ethanol, respectively, were directly pipetted to the membrane with the vacuum pump on. The flow-through was discarded. Afterwards, the column was placed on a fresh 2 ml collection tube and centrifuged at 20.000 xg for 3 minutes. To dry the membrane completely, the column was incubated at 56 °C for 10 min on a new 2 ml collection tube. Finally, to elute cfDNA from the membrane, 55 µl AVE buffer were applied to the center of the column placed in a clean 1,5 ml elution tube, incubated for 3 min at RT and centrifuged at 20.000 xg for one minute, resulting in an expected total volume of 50 µl.

2.6.2. CfDNA quality control

Before further molecular analysis of ctDNA, the quantity and quality of isolated cfDNA was tested. This will build the basis for comparison of both isolation methods.
Isolated cfDNA samples from -20°C were thawed at RT, vortexed for 5 s and shortly spun down before any handling.

2.6.2.1. Quantity

Quantus

The Quantus™ Fluorometer from Promega was used to quantify isolated cfDNA. As low concentrations are expected, 2 µl sample were added to 198 µl fluorescent dye

(QuantiFluor ONE dsDNA Dye, Promega) into PCR tubes. This mixture is incubated for 5 minutes in the dark, so that the fluorescent molecule can intercalate with the basepairs of the cfDNA. The emitted fluorescence in each sample was measured with the ONE-DNA protocol based on a standard curve generated once in a month with internal standard samples included in the kit. The results were documented in ng/µl. All concentrations were recorded on Microsoft Excel for further analysis.

qPCR

For examination of the minimum requirements needed for dPCR, a quantitative PCR (qPCR) was conducted for indirect determination of analyzable copy numbers in the isolated cfDNA.

Hence, we conducted the qPCR based on the *GAPDH* (Glycerinaldehyd-3-phosphat-Dehydrogenase) gene with an amplicon length of 157. The *GAPDH* gene encodes an enzyme involved in glycolysis and is therefore known to be expressed in all human cells equally. For each run, a standard curve with 8 standards was generated starting with 14.500 copies/µl and a dilution series of 1:3. For every sample to be tested, 10 µl master mix (TaqMan ® Fast Advanced Master Mix, Applied Biosystems), 1 µl assay (GAPDH157 Applied Biosystems), 8 µl water and 1 µl DNA template were mixed. No template control was conducted with nuclease-free water only. The capillaries for quantification were placed on pre-cooled adapters, filled with the respected samples, centrifuged at 800x g for 10 sec and placed in the LightCycler 2.0 (Roche). The cycling conditions were as follows: 50 °C for 2 min, 95°C for 20 sec and (45x) 95°C 10 sec plus 60°C for 30 sec. The resulting Ct values, described as the cycle number where the PCR curve crosses the threshold in the linear part of the curve, were compared to the standards by the software resulting in indirect quantity value of cfDNA in copies/µl. All results were documented on Microsoft Excel.

2.6.2.2. Quality - Fragment length

To prove the integrity of the isolated cfDNA, we conducted an analysis of the fragments´ lengths of selected samples with sufficient DNA quantity using the Agilent High Sensitivity DNA Kit from Agilent Technologies.

This kit is designed for total DNA in the sample between 5 – 500 pg/µl and ranges sizes between 50 – 7000 bp. First, the gel-dye mix was prepared mixing 15 µl High Sensitivity DNA dye and into the High Sensitivity DNA gel matrix. The solution was transferred to a filter and centrifuged at 2240 x g for 15 minutes.

Nine microliters of the prepared gel-dye mix were loaded on a High Sensitivity DNA Chip (Agilent Technologies) using the Chip Priming Station (Agilent Technologies). The rest of the gel-dye mix was stored at 4 °C for further usage within 6 weeks after preparation. Next, 5 µl of the marker solution containing the lower marker at 35 bp and a higher marker at 10380 bp was loaded into all sample and ladder wells. One microliter High Sensitivity Ladder as well as 1 µl of each sample were loaded on the chip. Unused wells without DNA were filled with an additional microliter of marker.
The final chip was horizontally vortexed for a minute at 2400 rpm (IKA® MS 3 Vortexer), checked for bubbles and ran on the Agilent 2100 Bioanalyzer instrument within 5 minutes.

2.6.3. CtDNA detection – targeted hotspot variant analysis using dPCR

As described above, dPCR is a highly sensitive and specific method that enables quantification of short ctDNA fragments. First, the sample is portioned in 20.000 single reactions before amplification. Second, small amplicons are generated using a dPCR assay designed for each mutation. The resulting products are quantified through the detection of fluorescent mutation-specific probes. Informative mutations and wildtype alleles are identified by FAM-positive and VIC- positive signals, respectively. A schematic representation is shown in Figure 3.

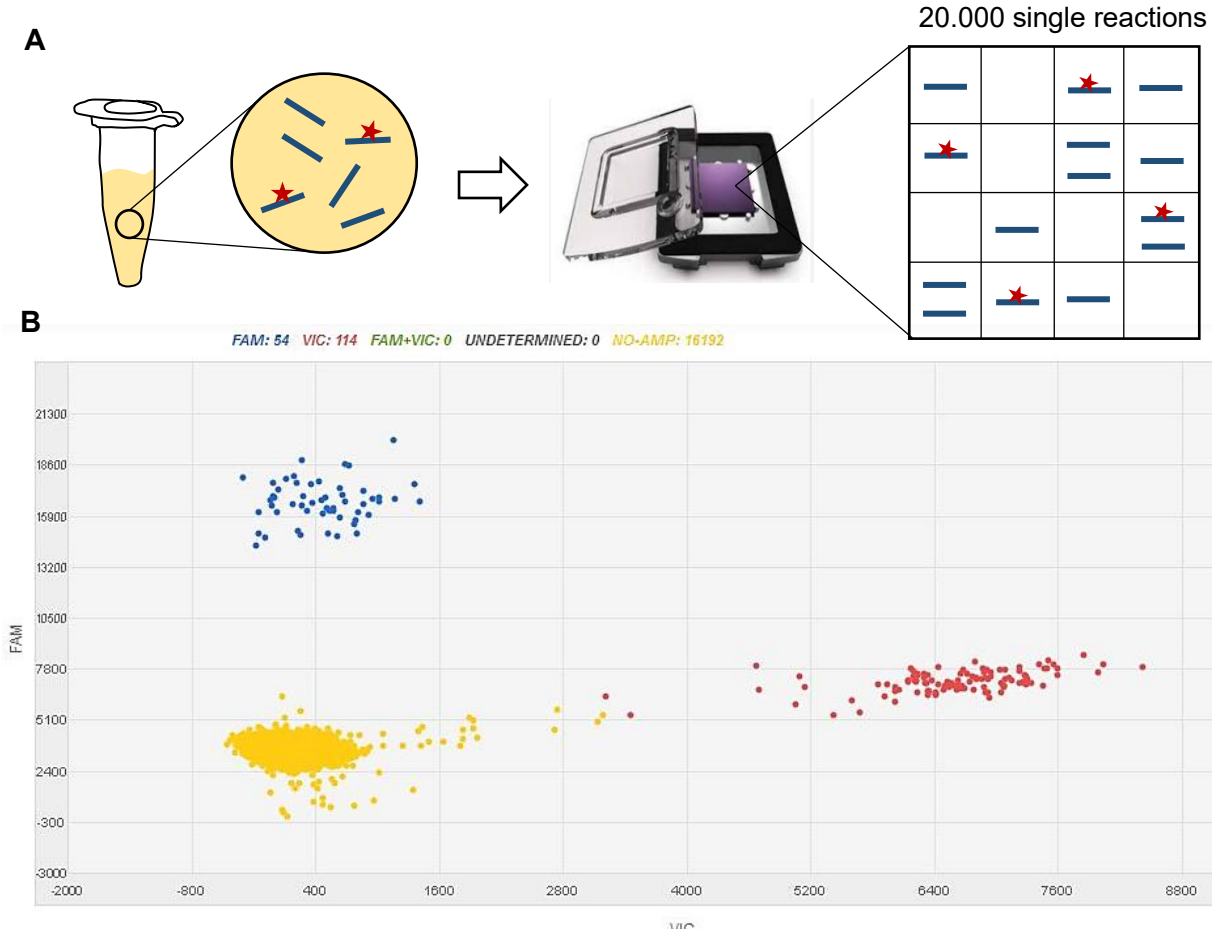

Figure 4: Overview of the dPCR system from Applied Biosystems

A – Isolated cfDNA containing tumor-specific ctDNA with characteristic mutations is applied onto a chip with 20.000 micro chambers. Thus amplification occurs in 20.000 single reactions resulting in a digital [0; 1] result with a positive or a negative signal for the tagged mutation.
B – The fluorescent mutation-specific probes emit a positive signal in the FAM channel (blue dots), whereas wildtype alleles appear positive in the VIC signal (red dots). Empty chambers show no amplification (NO-AMP) and are depicted as yellow dots.

Here, we used the QuantStudio 3D Digital PCR System from Applied Biosystems. The PCR mix consisted of 17,4 µl universal MasterMix (QuantStudio™ 3D Digital PCR Master Mix v2, Applied Biosystems), 1,74 µl of each assay and 15,66 µl cfDNA. Each dPCR was carried out in duplicates with a reaction volume of 14,5 µl each and loaded into dPCR chips (QuantStudio™ 3D Digital PCR 20K Chip, Applied Biosystems) by the Chip Loader (QuantStudio 3D Digital PCR Chip Loader, Applied Biosystems). The loader guarantees even application of the sample on the chip, so that DNA molecules are dispersed equally into the 20.000 microchambers. Genomic DNA of FFPE material from primary tumors with known mutations were used as positive controls. No template controls were performed with nuclease-free water only. PCR was conducted on the ProFlex™ PCR System Dual Flat Block Thermal Cycler (Applied Biosystems). The

thermal cycling conditions were as follows: 96 °C for 10 min, 56 °C for 2 min, 98 °C for 30 s then 60 °C for 2 min. After PCR, chips were read by the ChipReader (QuantStudio 3D, Applied Biosystems), interpreted by QuantStudio™ 3D AnalysisSuite Cloud Software (ThermoFisher) and exported into Microsoft Excel for further analysis.
Percentages of mutated alleles, as reported in the results, consist of the mean detected targets per total detected alleles of the duplicates run.

2.7. Statistical Analysis

Statistical analysis were performed using RStudio. All data are presented as mean values. Comparison between two groups was conducted using the Wilcoxon-Test. Pairwise correlation of presurgical parameters was performed based on Pearson correlation with p-values generated using the R package *Hmisc* and visualized with the package *corrplot*. Hierarchical agglomerative clustering was evaluated using the *hclust* function (method= “complete”). Disease-free survival (DFS) was analyzed based on the log-rank test using the R package *survminer* and visualized by the Kaplan-Meier method. In general, p-values under 0.05 were considered statistically significant.

3. Results

3.1. Establishing a protocol for ctDNA assessment by dPCR

3.1.1. Analyzable copy numbers depending on plasma input

First, the volume needed from a blood draw for reliable cfDNA isolation was examined. Blood draws in 9 ml EDTA tubes were obtained from cancer patients in the clinical routine resulting in up to 4 ml plasma per sample available. Therefore, cfDNA quantity was analyzed in one to four ml plasma (Figure 5).

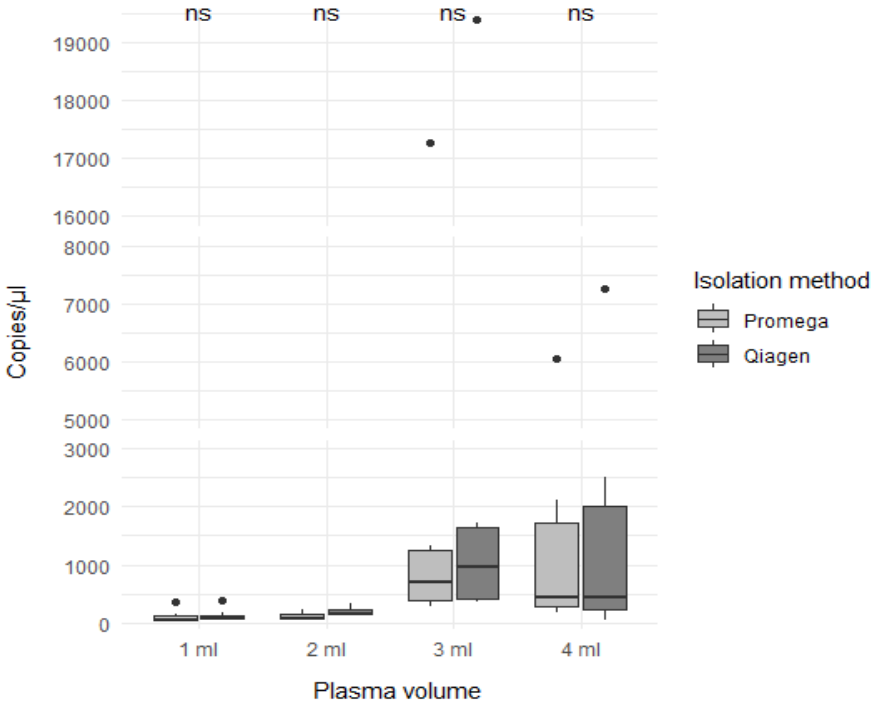

Figure 5: Boxplots of ctDNA quantity depending on plasma volume

CfDNA was isolated using two different protocols (Promega and Qiagen). Quantity was measured by Quantus and documented as copies/µl in elution. Box limits indicate the interquartile range (IQR) from the 25th percentile to the 75th percentile. Central lines mark the median value. Lower and upper whiskers depict the minimum and maximum values, respectively. The higher the plasma input, the higher the isolated cfDNA amount. Comparison of the two isolation methods was conducted using the Wilcoxon-test. No statistical significance can be detected between the two methods at any isolation volume. Ns: not significant

CfDNA isolation with both methods (Promega and Qiagen) were considered separately to ensure that quantity differences are solely based on input variations. Within each group, plasma samples were isolated in parallel. Not all cancer patients contributed equally to the four categories (one to four ml plasma). For instance, the outliers at three-

and four-ml plasma stem from two different individuals. DNA quantity was measured fluorometrically by Quantus and recorded as copies/µl in elution. As expected, the mount of cfDNA correlates positively with the plasma input. The highest mean values can be observed at a total plasma volume of four ml with an average of 686 (Promega) and 762 (Qiagen) copies/µl cfDNA. Although the median cfDNA quantity of isolation from 4 ml plasma is lower than from 3 ml (709 – 975 copies/µl from 3 ml vs. 434 – 436 copies/µl from 4 ml plasma), these results show overall greater variance due to inter-patient deviations.No statistical differences can be observed between both isolation methods independently from the plasma volume used.

As described above, cfDNA is highly fragmented compared to genomic DNA. To validate analyzable copy numbers in cfDNA for latter dPCR, we conducted a qPCR designed for an amplicon length of 157 bp from material isolated from 3 and 4 ml plasma (Figure 6).

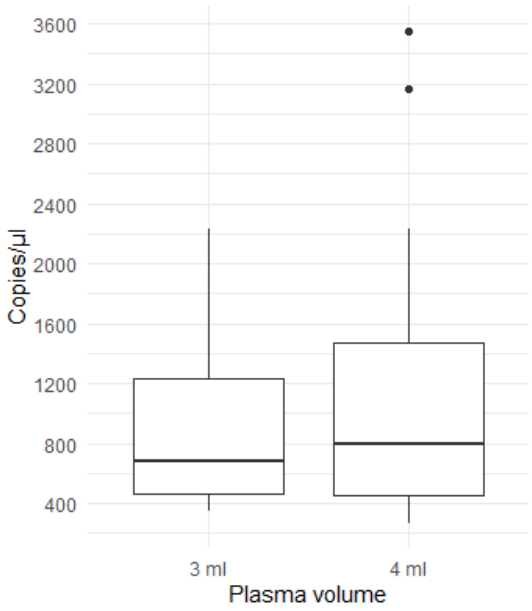

Figure 6: Validation of analyzable copy numbers in cfDNA by qPCR

Boxplots of cfDNA quantity in copies per µl elution as measured by qPCR from 3 and 4 ml plasma. Box limits indicate the interquartile range (IQR) from the 25th percentile to the 75th percentile. Central lines mark the median value. Lower and upper whiskers depict the minimum and maximum values, respectively.
qPCR: quantitative PCR

Here the results include samples processed with both protocols. As measured by qPCR, cfDNA isolation from 3 ml plasma enables detection of 678 copies. Additional plasma volume increases this value to 801 copies/µl. Regarding the input volume of 14,5 µl for dPCR, 9.831 copies can be analyzed in total within one assay after cfDNA isolation from

3 ml plasma while isolation from 4 ml allows examination of 11.614 copies in a dPCR run.

Absolute quantification using qPCR as designed here with a fragment length similar to cfDNA, gives an accurate glimpse of molecules amplifiable in the following dPCR reaction. However, it is, compared to Quantus, a time expensive method. The Quantus system quantifies DNA fluorometrically and is therefore independent of cfDNA length. Given the fact that measurements with Quantus require less hands-on time for the routine, the correlation between both quantification methods was examined (Figure 7). Here, the results show a good correlation between both quantification methods (R^2= 0,8798) within all samples tested (3- and 4- ml isolated samples).

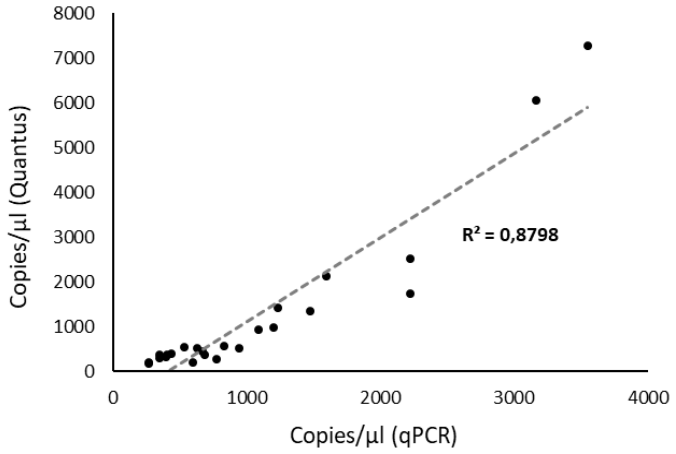

Figure 7: Correlation of two methods for cfDNA quantification

Scatterplot of detected copies cfDNA per µl elution isolated from 3 and 4 ml plasma measured with qPCR (X-axsis) and the Quantus system (y-axis). Dashed line represents the linear trend line. The variation of the dependent variable as predicted from the independent variable is described by the coefficient of determination R^2

Taken together, isolating cfDNA from the highest volume possible (4 ml plasma from a 9 ml blood draw) results in the most amount of DNA for further analysis. For the routine, cfDNA can be quantified reliably using the Quantus system.

3.1.2. Impact of applied cfDNA isolation protocol

Next, in order to further examine the efficiency of each isolation protocol, the number of copies per µl detectable in four ml plasma was examined based on Quantus and dPCR (Figure 8).

Here, samples from six individuals isolated with both protocols were analyzed with both methods (Quantus and dPCR) in parallel. The outliers stem from the same patient. The measured copy numbers show great variances independently of the isolation and detection method. As described above, no significant differences can be detected in the fluorometric quantification. The median copies per µl as detected by dPCR are 214 and 198 for Promega- and Qiagen isolation, respectively. These values are almost half of the copies as detected fluorometrically (434 copies/ µl with Promega and 436 with Qiagen). This effect was expected, as dPCR is a targeted approach based on DNA amplification of a specific region while the Quantus system measures all DNA fragments equally.

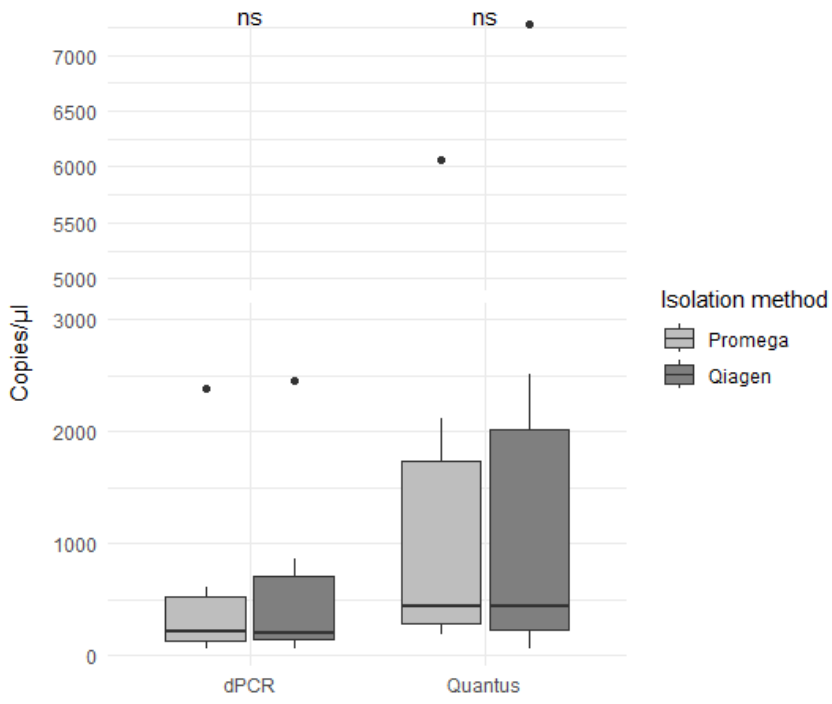

Figure 8: Copy number measured with Quantus and dPCR depending on the applied isolation protocol

CfDNA was isolated from 4 ml plasma using both protocols (Promega and Qiagen). Quantity was measured by Quantus and dPCR and documented as copies/µl in elution. Box limits indicate the interquartile range (IQR) from the 25th percentile to the 75th percentile. Central lines mark the median value. Lower and upper whiskers depict the minimum and maximum values, respectively. Comparison of the two isolation methods was conducted using the Wilcoxon-test. No statistical significance can be detected between the two isolation methods either based on Quantus nor dPCR.
dPCR: digital PCR; Ns: not significant

Independently from the testing method, Promega and Qiagen show no significant differences in the isolation efficiency.

Furthermore, cfDNA integrity, with respect to fragment length, was examined for both isolation methods (Figure 9). As described above, cfDNA is described to appear in a length of 150-180 bp corresponding to the mononucleosomal DNA in eukaryotic cells. Examination of fragment length using the Bioanalyzer system was tested from samples with sufficient cfDNA quantity. Material was obtained from different patients isolated with each of the two protocols, Promega (A) and Qiagen (B). Both results exhibit the spiked in markers at 35 and 10380 bp and show low background noise. The peaks´ height reflects DNA quantity which is sample-dependent and was not adjusted for the assay. Both isolation methods show defined peaks within the expected range (Promega at 175 bp and Qiagen at 163 bp). Smaller peaks are visible, especially in the Qiagen-isolated

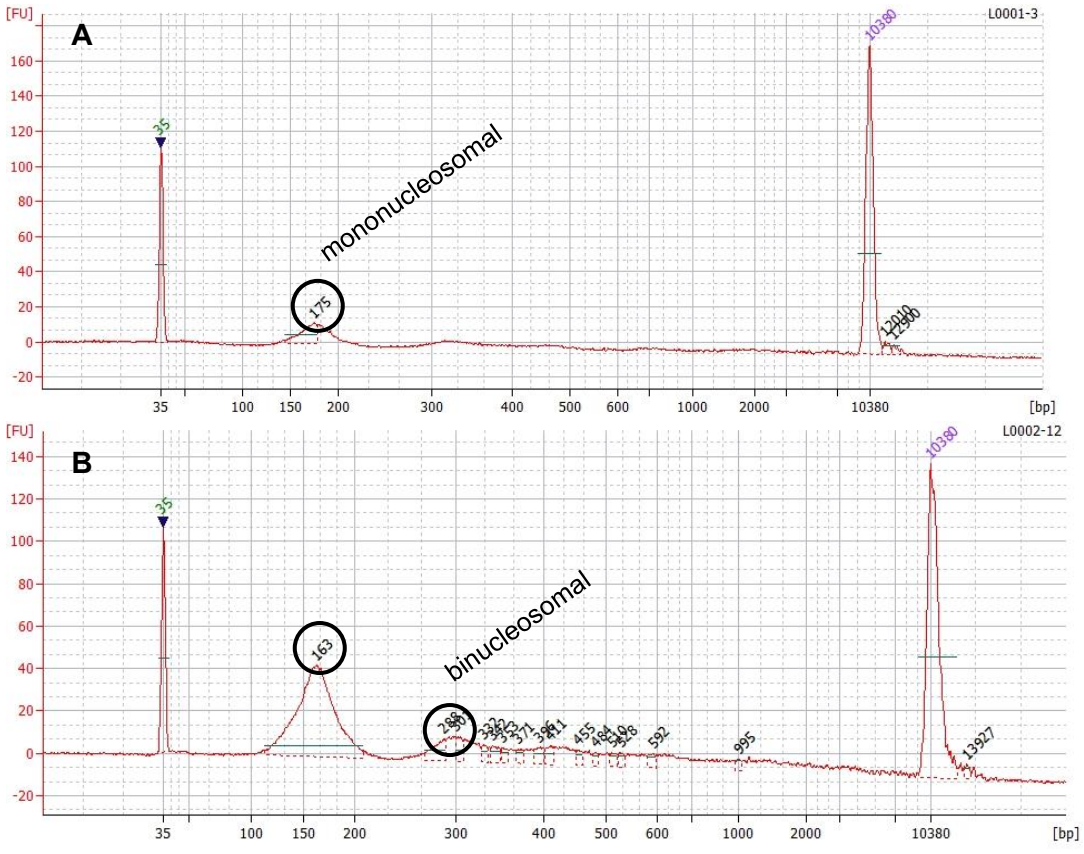

Figure 9: Electropherogram of isolated cfDNA after isolation with both protocols

A: Promega-, B: Qiagen-isolation
X axis is shown in basepairs (bp) of DNA fragments and y axis as fluorescent units (FU). The peaks visible at 35 and 10380 depict the lower and upper marker as controls for an overall successful run. Distinct peaks at 175 bp (A) and 163 bp (B) correspond to the isolated cfDNA.

sample, at around 300 bp. Fragments with lengths of multiples of the expected 150-180 bp can be interpreted as di- tri-nucleosomes and long fragment cfDNA.

3.1.3. DPCR limit of detection (LoD) and reproducibility

Digital PCR is described to be a highly sensitive method for mutation detection down to 0,1% mutated alleles. To establish the LoD for the routinely analysis of LBx in the clinical context, we used first, commercially available DNA and second, cfDNA isolated from a patient with a known *KRAS* mutation (Figure 10).

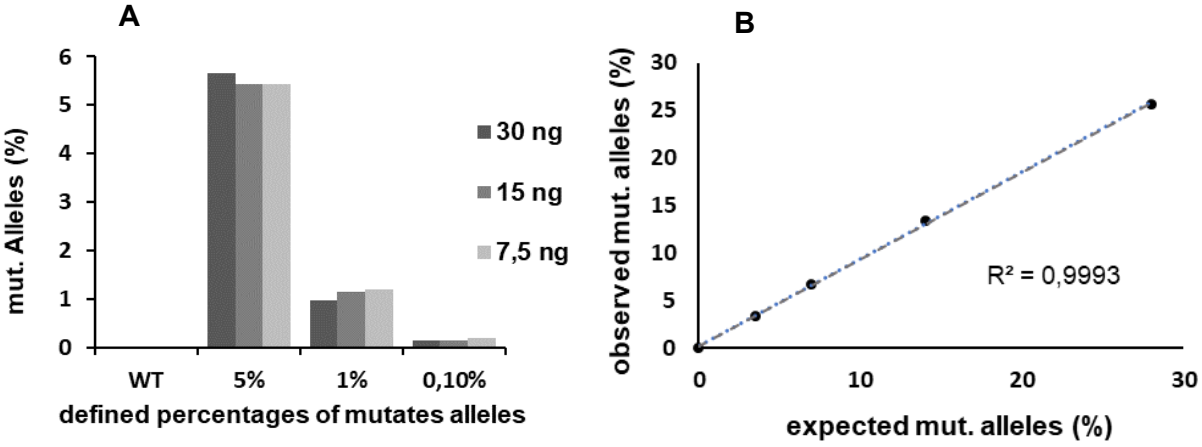

Figure 10: Testing the limit of detection (LoD) and reproducibility of dPCR: Testing the limit of detection (LoD) and reproducibility of dPCR

A- Defined percentages of the *EGFR* mutation T790M were analyzed by dPCR with different DNA inputs. The results are shown as detected percentages of mutated alleles (y-axis).

B- Correlation of the observed and expected results of a dilution series of *KRAS* positive cfDNA with wildtype cfDNA as measured by dPCR.
The variation of the dependent variable as predicted from the independent variable is described by the coefficient of determination R^2.

Mut.: mutated; WT: wild-type (DNA)

Firstly, we conducted dPCRs of genomic DNA (Horizon Discovery) with spiked in defined percentages (5%, 1%, 0,1%) of the *EGFR* mutation at the p.T790M hotspot. WtDNA without genetic alteration was used as a negative control (WT). All samples were loaded with 30, 15 and 7,5 ng DNA each and the dilutions were conducted by reduced volume input. Independently from DNA quantity, there was no signal of amplification of mutated alleles in any wild-type sample. The detection rates of the expected 5% and 1% samples display 5,1 – 5,4 % and 1,0 – 1,2 % mutated alleles, respectively. As for the specimen

with an expected mutation rate of 0,1 %, the dPCRs resulted in 0,15 %, 0,16 % and 0,2% for 30, 15 and 7,5 ng DNA, respectively, showing a higher inaccuracy the lower the input. To examine reproducibility, the 0,1% assay with 30 ng DNA input was replicated. Here, the results again depicted 0,15 % (CI: 0,06% - 0,36%) mutated alleles.

To transfer the LoD characterization to cfDNA, we performed analysis of a dilution series of cfDNA from a patient with a known *KRAS* mutation at the p.G13D hotspot of 30% with wild type cfDNA of a healthy donor. The rerun of the undiluted initial sample resulted in 26 % mutated alleles (CI: 20,343% - 32,236%). After four dilution steps, the outcomes to be expected were 15%, 7,5%, 3,75% and 1,9%. Comparable to the undiluted sample, the observed results of the first three dilutions steps were overall lower than expected with 13%, 6,7% and 3,3% while the 1:16 dilution resulted in 2,6% mutated alleles (0,7 % higher than expected). Furthermore, we executed an extra dilution of 1 to 128 (0,23% expected mutated alleles) to test the LoD in the context of cfDNA. Here, the outcome was 0,7 % (CI: 0,133% - 4,461%).As shown in figure 9B, the observed patterns of the dilution series from dPCR analysis correlate highly with the expected ratios (R^2= 0,9993). Taken together, these results show high reproducibility of dPCR for different DNA inputs as well as in the general context of cfDNA and a possible LoD of 0,1%.

3.2. NeoRect trial

3.2.1. Patient population and tumor characteristics

Within two years, a total of 40 patients diagnosed with locally advanced RC at the University hospital of Augsburg were included into the NeoRect trial (Figure 11). Five of the patients included stopped the protocol at an early stage (four of them due to personal decision and one being diagnosed with an alternative cancer entity before treatment initiation) and seven had an external TME, so that neither final staging, nor LBx, nor RS were available for analysis.

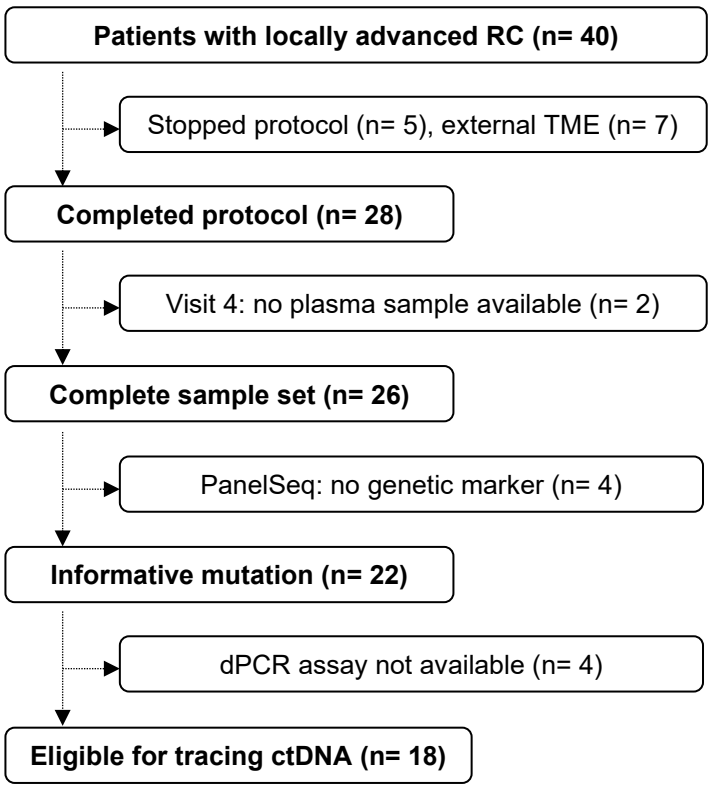

Figure 11: Consort diagram of patients included in the NeoRect trial

From the 40 patients intended to treat, 26 had a complete data set after surgery. Due to technical limitations, 18 individuals were eligible for tracing ctDNA in plasma samples.

From the 28 participants who completed the protocol, two individuals missed blood draw before surgery (V4), resulting in 26 individuals with a complete sample and data set. As we focused on single hotspot mutations for LBx, detection of an informative mutation in the tissue biopsies is crucial. This was not given for four patients. Furthermore, analysis with dPCR depends on commercially available assays, which are not accessible for all

possible mutations. Due to these methodological limitations, there was a total of 18 patients eligible for ctDNA tracing in our trial. An overview of patients´ characteristics of the population intended to treat is shown in table 7.

Table 7: Patient characteristics at diagnosis of the population in the NeoRect trial

Intent to treat (n=40)		
Age		(%)
Median (Range)	68 (37-87)	
Sex		
Male	29	73
Female	11	28
cm a.a. (min)		
Median (Range)	7 (0,1-11)	
cT		
2	2	5
3	29	73
4	9	23
cN		
0	6	15
1	11	28
2	17	43
+	5	13
x	1	3
G		
2	30	75
3	2	5
x	8	20
cM		
0	34	85
1	6	15

a.a: ab ano
cT / cN / cM: clinical assessment data
T: Tumor
N: Nodes
G: Grading
M: Metastases

Individuals included into the trial were between 37 and 87 years old and 73% were male. The median tumor´s minimal distance ab ano measured by rectoscopy was 7 cm. Although nine individuals were described as tumor stage T4, which includes tumor cells growing through the wall into nearby organs, only six patients showed distant metastases (four in the liver, one in the lungs and one in both, liver and lung). Tumor stage T3 was diagnosed most frequently in our trial (73 %). The number of nearby affected lymph nodes varied greatly in the cohort (none to up to more than 7). Five were described as generally positive but without a specific number and in one case an infestation of lymph nodes was suspected but not finally confirmed. In this population the majority was histopathologically classified as G2 (moderate grade; 75%) meaning cancer cells appeared moderately differentiated and looked abnormal. For eight individuals no grading was available.

Among the 40 patients included into the trial, 28 participants completed the protocol with surgery at the University hospital Augsburg allowing full classification of the tumor specimen after TME. (Table 8)

Table 8:Tumor characteristics after surgery of individuals with a complete protocol

complete protocol (n=28)		
ypT		(%)
0	4	14
1	2	7
2	11	39
3	9	32
4	2	7
ypN		
0	19	68
1	6	21
2	2	7
3	1	4
L		
0	26	93
1	2	7
V		
0	22	79
1	6	21
Pn		
0	23	82
1	5	18
R		
0	27	96
1	1	4
M		
0	22	79
1	6	21
G		
2	23	82
3	1	4
x	4	14
Dworak		
1	2	7
2	19	68
3	5	18
4	2	7

ypT / ypN: pathological data following therapy
T: Tumour
N: Nodes
L: Lymph vessels
V: Veins
Pn: Perineural tissue
R: Resection edge
M: Metastases
G: Grading

Here, both, ypT and ypN staging, vary considerably. In four patients no remaining evidence of primary tumor in the area resected was observed (ypT0). Three of these had been described as T3 and one as T2 at the time of diagnosis. Both patients classified as ypT1 were described in all other categories with zero but showed tumor cells moderately differentiated (G2). The majority of the patients (71%) were ranked higher as ypT2 or

ypT3 after nRCT. Only two samples were categorized as resistant tumors (ypT4) after therapy and resection, one from a patient initially also ranked as T4 and one described as T3 before treatment. The majority of the patients showed a negative nodal status after therapy (68%), independently from the amount of positive assessed lymph nodes at the time of diagnosis. Individuals classified ypN1 or ypN2 (n=8) were ranked equally or lower before therapy, while the patient described to be ypN3 after therapy was reported as N2 at diagnosis, meaning that more lymph nodes seem to have been affected by the tumor during treatment. Most of the resected specimen showed neither invasion in lymph vessels (L0, 93%), nor in veins (V0, 79%) nor in perineural tissue (Pn0, 82%). In one case, although the tumor was macroscopically fully resected, small tumor residuals were detectable histopathologically at the resection edge (R1). Interestingly, two of the six patients with detectable distant metastases in the liver after treatment (M1) had none (M0) at the time of diagnosis indicating tumor progression during nCRT. The distribution of the grading is similar before and after surgery with most being classified as G2 (n= 23) and one as G3.

Based on the pathologic features, the specimens were classified into Dworak scores from one to four. Two individuals were ranked with a Dworak score 1 concordant with high ypT values (ypT3). Dworak score 2, interpreted as easy to find single or groups of tumor cells, was described most frequently with 68%. Eighteen percent of the resected specimens were categorized as Dworak 3 with only few and hard to find tumor cells in mostly fibrosed tissue. Within the group with a Dworak 3 scoring, one individual was pathologically described as a subtotal remission, as there was no sign of residual primary tumor (ypT 0), but few regional lymph nodes metastasized (ypN 1). A complete tumor regression in terms of no tumor cells but only fibrosis in the specimen (Dworak 4) was reported in two individuals, both classified as T3 primary tumors at the time of diagnosis.

3.2.2. Molecular analysis of primary tumor

Panel sequencing of primary biopsy was performed for all participants for molecular analysis of activating mutations in the context of the standard management. Furthermore, with the intention to conduct dPCR of plasma samples, sequencing beforehand gives information about potentially traceable mutations for the dPCR assay. An overview of the detected mutations in shown in figure 12.

From the forty patients included, three individuals weren´t sequenced due to missing primary biopsy (P02, P19 and P28). P40 had also no primary material available at the time of diagnosis but was molecularly examined by NGS after resection - here a *KRAS*

mutation could be detected. A total of 21 relevant somatic mutations were described ranging from 1 to 9 mutations per patient. Three individuals showed no mutational patterns in the analyzed genes (P27, P30, P32) and eight patients pictured only one mutation each.

The given percentages between 2% and 62% depict the frequencies of the aberrated

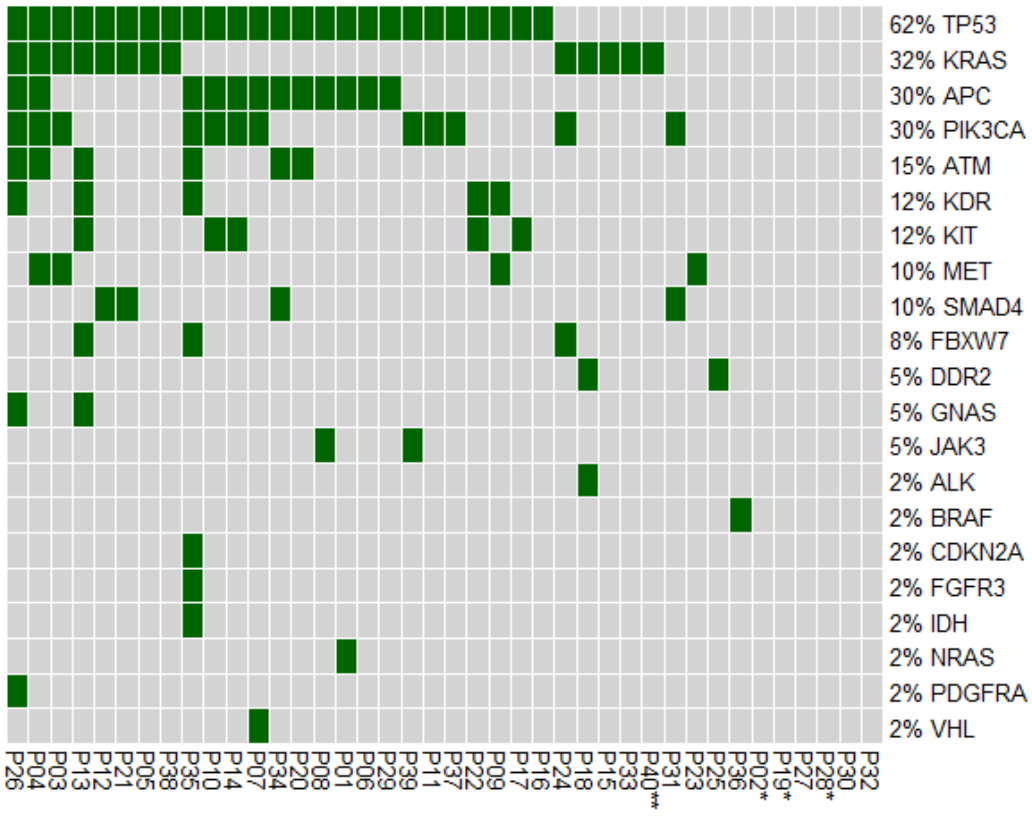

Figure 12: Detected mutations by next generation sequencing of all patients included into the trial (n=40)

Twenty-one mutations were detected in total by NGS. Between 2% and 62% of the samples were positive for each mutation within the NeoRect cohort of 40 patients.
* no NGS data available
** Sequencing after resection

genes in the cohort and include different types of modifications within each hotspot. The most commonly mutated gene was at the *TP53* hotspot (62%) followed by a high ratio of *KRAS* mutations (32%) as it is known to occur frequently in rectal cancer. As described above, the *APC* and *PIK3CA* genes were also expected to be aberrated often. In our cohort, they each appear mutated in 30% of the cases. *BRAF* and *NRAS* mutations were lowly represented with only one positive patient each (2%).

From these mutational patterns detected by NGS, one aberration was selected for each patient eligible for ctDNA analysis (n=18) based on high VAFs in primary tumor to trace the biggest clonal proportion and the availability of a commercial assay for dPCR.
The VAFs of the selected mutations varied between 2,7% and 79% (Figure 13). However, the very low frequency of 2,7% corresponds to the sequenced material of P40 after resection and nCRT. This *KRAS* mutation couldn´t be identified in primary tissue at the time of diagnosis neither by NGS nor retrospectively by dPCR appearing to have arisen during the course of therapy. In the other 17 patients the VAFs of the corresponding mutations were above 10%.

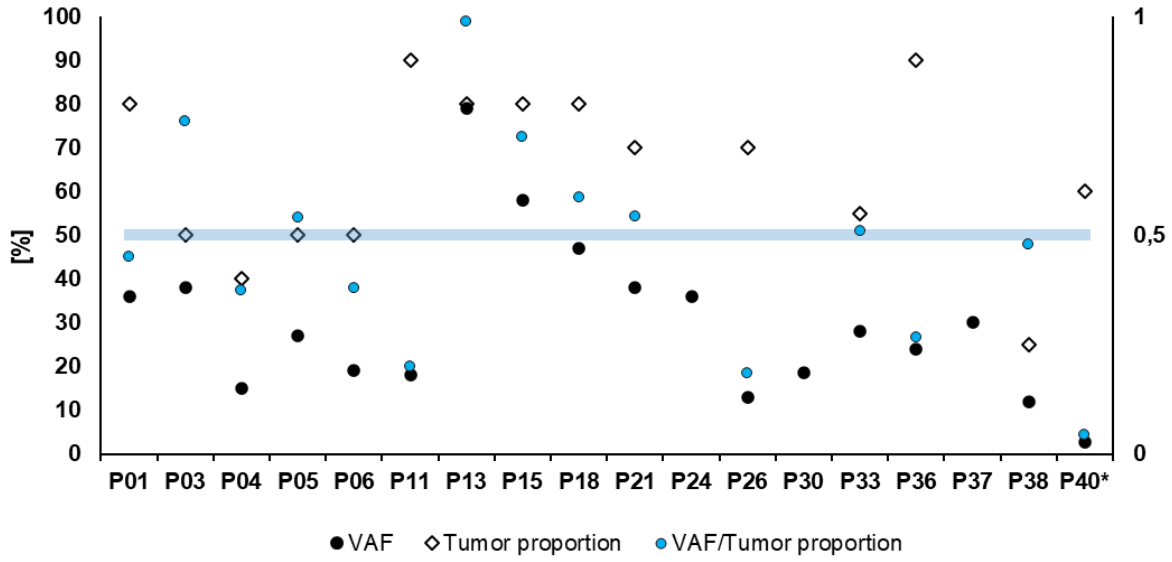

Figure 13: Tumor proportions and variant allele frequencies (VAF) of mutations selected for ctDNA tracing (n=18)

Tumor proportion as described by pathologists (white dots) and VAFs from NGS (black dots) are depicted in percentages. Blue dots show the quotients of VAFs and tumor proportions. The blue line indicates a quotient of 0,5 as expected if all tumor cells in the microdissected area are positive for the selected mutation.
*Sequencing after resection; VAF= variant allele frequency

Regarding the tumor proportions as described by the pathologists in the areas microdissected for NGS, the values varied between 25% and 90% (mean 70%). In three participants this information was not recorded (P24, P30, P37). If possible, the main clone, defined as all (or most) tumor cells harbouring the same specific mutation, was chosen for dPCR tracing. In this case, a proportion of 0,5 (blue line) between VAFs and tumor proportion is expected, meaning that one allele is mutated per tumor cell. The blue dots in figure 12 show this quotient for each patient. Under the premise of heterozygosity without allelic loss or deletions, values under 0,5 imply that not the main clone was

chosen. This effect is most clear in P40, where the mutation arises during therapy, as described above. The other extreme can be observed in P13. Here the quotient of VAF and tumor proportion results in one. This can be interpreted as either both alleles being mutated in all tumor cells or, more likely, a loss of the corresponding unmutated allele. A list of the selected mutations for each patient is shown in table 9.

Table 9:Selected mutations for dPCR tracing according to the Catalogue Of Somatic Mutations In Cancer (COSMIC)

Patient ID	Gene name	CDS mutation	AA mutation	Legacy Identifier (COSMIC)
P01	*NRAS*	c.182A>G	p.Q61R	COSM584
P03	*KRAS*	c.34G>A	p.G12S	COSM517
P04	*KRAS*	c.35G>T	p.G12V	COSM520
P05	*KRAS*	c.35G>A	p.G12D	COSM521
P06	*TP53*	c.844C>T	p.R282W	COSM10704
P11	*PIK3CA*	c.1633G>A	p.E545K	COSM763
P13	*KRAS*	c.436G>A	p.A146T	COSM19404
P15	*KRAS*	c.436G>A	p.A146T	COSM19404
P18	*KRAS*	c.437C>T	p.A146V	COSM19900
P21	*TP53*	c.743G>A	p.R248Q	COSM10662
P24	*KRAS*	c.34G>T	p.G12C	COSM516
P26	*PIK3CA*	c.1633G>A	p.E545K	COSM763
P30	*KRAS*	c.436G>A	p.A146T	COSM19404
P33	*KRAS*	c.35G>T	p.G12V	COSM520
P36	*BRAF*	c.1799A>T	p.V600E	COSM476
P37	*PIK3CA*	c.3140A>G	p.H1047R	COSM775
P38	*KRAS*	c.35G>A	p.G12D	COSM521
P40	*KRAS*	c.34G>C	p.G12R	COSM518

ID: Patients identification number of NeoRect trial
CDS: Coding sequence
AA: Amino acids
COSMIC: Catalogue of somatic mutations in cancer

Eleven of the eligible individuals were traced by *KRAS* mutations on different hotspots. The *NRAS* and *BRAF* mutations detected were used for the corresponding patients to track ctDNA. Moreover, three participants were tracked by *PIK3CA* mutations, two of them sharing the same assay at the p.E545K hotspot. Although *TP53* mutations were detected most frequently in our cohort (62%) it was used as a dPCR assay only in two cases, as most of the sequenced alterations in this gene appeared in non-hotspot

regions not known to be oncogenic and with about 50% VAFs suggesting them to be mostly germline mutations in one allele instead of tumor specific somatic aberrations.

3.2.3. Analysis of cfDNA in trial patients

First, we evaluated the levels of cfDNA in all patients eligible for tracing ctDNA (n=18) during the course of treatment (V1 – V4) and the respective proportions of ctDNA positivity over time. (Figure 14).

Within the eighteen individuals with complete data sets, cfDNA quantity increased during therapy peaking at visit 3 (V3) with 6,6 ng cfDNA per ml plasma (Range: 3,1 – 22,8 ng/ml). Measurements a day before surgery (V4) depict a slight decrement (median: 6,0 ng/ml).(Figure 14 A)

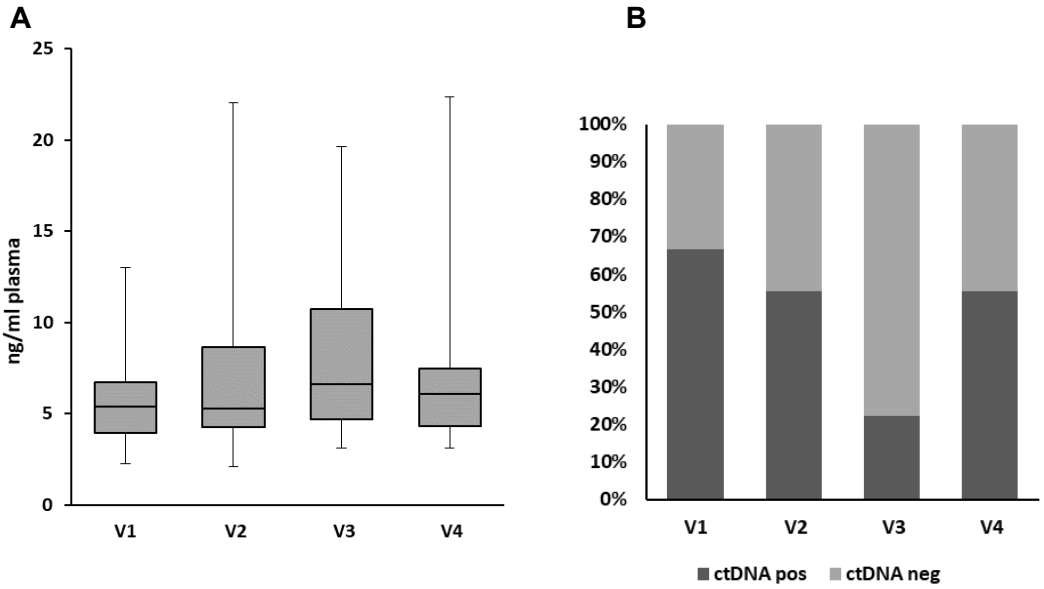

Figure 14 Analysis of LBx of patients with a complete data set and eligible for tracing ctDNA (n=18)

A- CfDNA quantity measured in ng/ml plasma in each of the visits during our trial
Box limits indicate the interquartile range (IQR) from the 25th percentile to the 75th percentile. Central lines mark the median value. Lower and upper whiskers depict the minimum and maximum values, respectively.

B- Proportions of ctDNA positive results during each visit.
Dark grey: ctDNA was detectable in plasma by dPCR (ctDNA pos); light grey: ctDNA was not detectable in the dPCR analysis (ctDNA neg)

Interestingly, ctDNA dynamics behave contrary. The highest ctDNA proportion can be observed at baseline (V1) before starting nCRT. Here, in two-thirds of the individuals ctDNA could be detected in plasma. Over the course of therapy, the number of positively

detected patients decreased to 55,6% at V2 and reaches the lowest value at the end of therapy (V3, 22%). In the interval between the end of nCRT and surgery ctDNA positivity rises again to over 50%, to the same level as in V2. (Figure 14 B)

3.2.4. ctDNA dynamics during nCRT

Next, ctDNA dynamics were analyzed at the individual patient level. Here, three main patterns can be observed (Figure 15). The first group is characterized by no ctDNA detection at any time point during or after therapy (A). Four of the five individuals in this

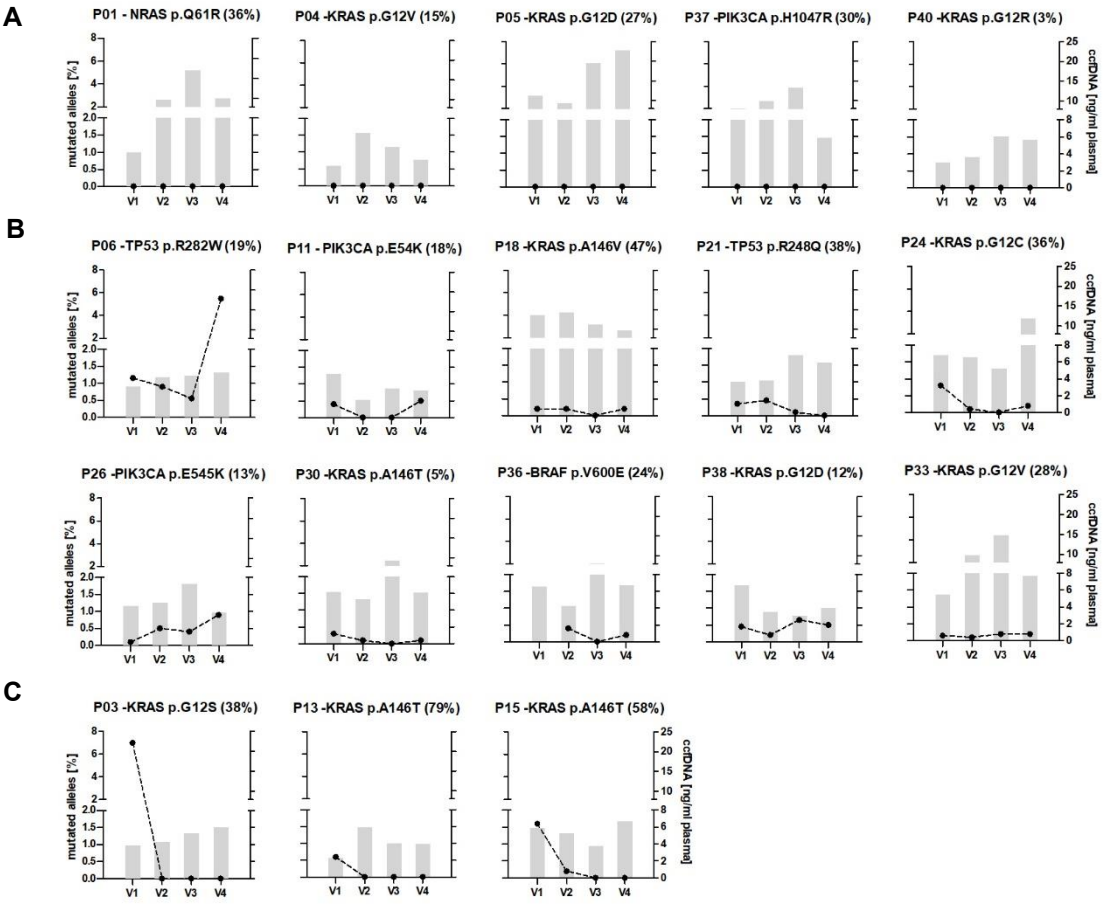

Figure 15: CtDNA and cfDNA dynamics during treatment for 18 patients with complete serial data available at all four time points of the NeoRect trial

Doted lines depict ctDNA dynamics as percentages of mutated alleles (left y-axis) and grey bars show cfDNA as ng/ml plasma (right y-axis). Individual headlines describe the patient ID of the NeoRect trial, its mutated gene and hotspot traced by dPCR as well as the VAFs detected by NGS from the initial biopsy in brackets.
Three groups can be defined based on ctDNA dynamics: Not detectable ctDNA at any time point (A), increment of ctDNA towards V4 compared to any timepoint during nCRT (B), and overall ctDNA decrement over the course of therapy (C).

group had *RAS* mutations (three *KRAS* and one *NRAS* mutation) in the respective biopsies ranging from 3% to 36% and one PIK3CA mutation. CfDNA levels were quite high in most of these patients, with the lowest at 5 ng/ ml plasma and the highest at 25 ng. It is to be noted, that P40 was traced by the *KRAS* mutation detected after resection, which could not be detected in the primary tissue sample. Therefore, its missing ctDNA values could be based on false negative results as the alteration seems to have arisen at a late stage of disease and in a very low represented subpopulation (3% VAFs in NGS).

The biggest group observed in our cohort contains 10 individuals (B). This cohort is defined by an increment of ctDNA in the interval between the end of nCRT and surgery. In this context, patients´ ctDNA cleared at a time point during therapy (V1 – V3) to no detectable or a very low level of ctDNA and increased again until V4. Three showed the lowest ctDNA level already at V2 while the majority reached the minimum by the end of nCRT (V3). Interestingly, unlike the observed steady decrement until the lowest level at V3, two individuals (P21 and P26) exhibit elevated ctDNA levels during therapy (V2) before dropping to a lower ctDNA level at V3. Participant P36 is missing a ctDNA value at V1 due to dPCR not being possible to evaluate but the increment between V3 and V4 allows its classification into this group. CfDNA quantity varies greatly within this group but is overall lower than in group A (mean $cfDNA_B$= 6,55 ng/ml plasma vs. mean $cfDNA_A$= 8,78 ng/ ml plasma).

The third group is characterized by constant ctDNA decrement (C). Two of these patients had only ctDNA detectable at the beginning of nCRT (V1) and one had positive ctDNA values until V2. By the end of therapy, no ctDNA can be detected and remains negative towards surgery (V4). Nevertheless, this group harbors the two individuals with the highest percentages of positively detected ctDNA at baseline (V1) (P03: 7% and P15: 1,6%). The overall measured cfDNA in this group in the lowest with a mean of 4,78 ng/ml plasma.

3.2.5. Association of ctDNA dynamics with response to therapy and other modalities

To evaluate the utility of ctDNA detection as a predictor of response to therapy, further modalities are taken into consideration - pathohistological classification after TME, MRI and rectoscopic response as well as the classic tumor marker CEA (Figure 16). Both, ctDNA group and ctDNA status before surgery as a single timepoint are considered.

Figure 16: Multimodal disease evaluation before and after surgery based on different clinical and pathological parameters and LBx (n=18)

Yellow: Pathological assessment after surgery (Remission status, Dworak score, ypT, ypN); Green: Clinical assessment before surgery (MRI, Rectoscopy, CEA value); Purple: LBx assessment (ctDNA group as described above, ctDNA value before surgery (V4))
pCR: pathological complete remission; SR: subtotal remission; CEA: Cancinoembryonic antigen

Within the 18 patients eligible for tracing ctDNA in our trial, only one was classified as a pCR after treatment (P01). This result is consistent with the MRI observations before surgery and CEA values within the physiological range. However, the individual was ranked to show “no response” in the rectoscopic assessment. This pattern is similar in the participant pathologically described with a subtotal remission (SR) status after TME (P04). Here, the MRI examination also revealed a good response while, again, the presurgical rectoscopic analysis underestimated the tumor´s response to therapy. Contrary to P01, the CEA values were elevated. Both P01 (pCR) and P04 (SR) had no ctDNA detectable at any timepoint. This is of special interest at baseline (V1), as the proportion of ctDNA negativity within this cohort is the lowest at this timepoint (33,3%). The three other members of this ctDNA group P05, P37 and P40 were described as no pathological responders. CtDNA negativity of P40 was discussed above. Nevertheless, CEA values and rectoscopy also suggest a good and MRI a moderate response to nCRT. Although finally classified as no pCR, P05 was ranked with a high Dworak scoring (Dworak 3) meaning there were only few and histologically hard to find viable tumor cells in mostly fibrosed tissue of the surgical specimen. This is concordant to the moderate response as observed by MRI. The last patient with no ctDNA detectable at any timepoint

P37 was described to have responded poorly to therapy in all presurgical modalities which was pathologically confirmed after TME (no pCR).

All other 13 patients were described to have no pCR. From these, 38,5% of the resctoscopic examinations before TME came to the conclusion of a good response after nCRT and 54% had physiological CEA values. The MRI assessment reported a poor response to treatment in only two cases. Remarkably, although three patients showed good responses to therapy in rectoscopic as well as radiographic assessment (P15, P21, P33) without elevated CEA values, remaining tumor cells could be histologically detected easily in the resected specimen (Dworak 2). Individuals of both groups, ctDNA increment and decrement, show no pathological remission after surgery. Interestingly, multimodal results vary greatly in the group of ctDNA decrement (P03, P13, P15). Whilst P13 is ranked with a high Dworak score of 3 but described to respond little in all presurgical modalities, P15 appeared to have a good response to therapy presurgically but could not be pathologically validated in the postsurgical specimen. Furthermore, P03 was the only participant reported as ypT 4 although rectoscopic assessment suggested a good response beforehand.

One category particularly stands out – ctDNA status before surgery compared to Dworak score. Statistical analysis based on Pearson´s Chi² test of the cross table shown in Table 10 confirms a significant correlation between these parameters (Chi² = 6.428571, d.f. = 1, p= 0.01123).

Table 10: Cross table between Dworak score and ctDNA status before surgery

		Dworak Score		
		1/2	**3/4**	Total
ctDNA preOP	**Pos**	10	0	10
	Neg	4	4	8
	Total	14	4	18

Furthermore, routinely obtained assessments as well as ctDNA before TME were further analyzed with the intention of recognizing potential correlations in-between presurgical parameters. (Figure 17). The highest correlations can be observed including CEA values. On the one hand, the assessment of presurgical CEA and rectoscopically defined tumor response show the highest correlation coefficient of 0.34. On the other hand, CEA and

ctDNA evaluation at V4 appear to correlate to the same extent but negatively (-0.34). In comparison, a smaller association can be observed of CEA values to MRI tumor assessment (0.21). In general, tumor responses as described by MRI depict lower correlations to all other modalities. Rectoscopic response and ctDNA before TME exhibit the lowest interdependence (-0.13). Taken together, although trends are recognizable, no correlation values can be observed above 0.34 such that only a weak connection between the parameters can be reported.

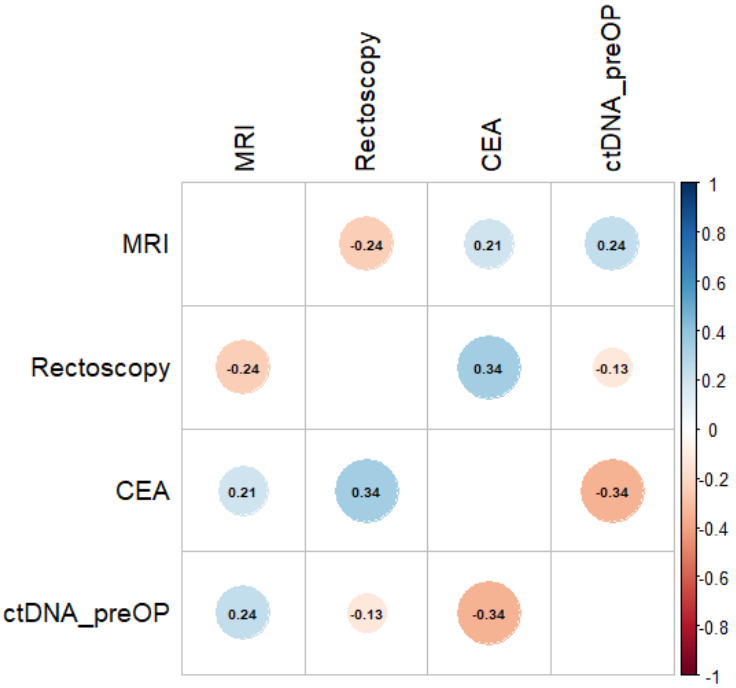

Figure 17: Pairwise correlation of presurgical clinical parameters and ctDNA evaluation before TME (V4)

Pearson correlation of assessed tumor response to therapy before surgery by MRI, resctoscopy and CEA in the context of routine presurgical evaluation and ctDNA detection at V4. MRI and rectoscopy were categorized as good or no response to therapy, CEA values as physiological (0-3,8 ng/ml) or elevated and ctDNA positive or negative. Missing values were ignored. Values within circles portray correlation coefficients. Blue depicts a positive and red a negative correlation, respectively.
CEA: Carcinoembryonic antigen; preOP: before surgery

As presurgical assessment methods appear to be independently of each other, points were distributed to form a scoring system to combine these parameters in order to allow prediction of tumor response to therapy. Zero points were assigned for a reported complete/good response in MRI and rectoscopy, physiological CEA values (0-3.8 ng/ml) and an observed ctDNA negativity before surgery. All other classifications (worse response), elevated CEA values and ctDNA positivity at V4 were ranked with 1 point.

This results in a scoring system ranging from 0 to 4 (the lower the score, the better the estimated pathological response) (Figure 18 A). The formed pre-surgical score was compared to the final Dworak score (Figure 18 B).

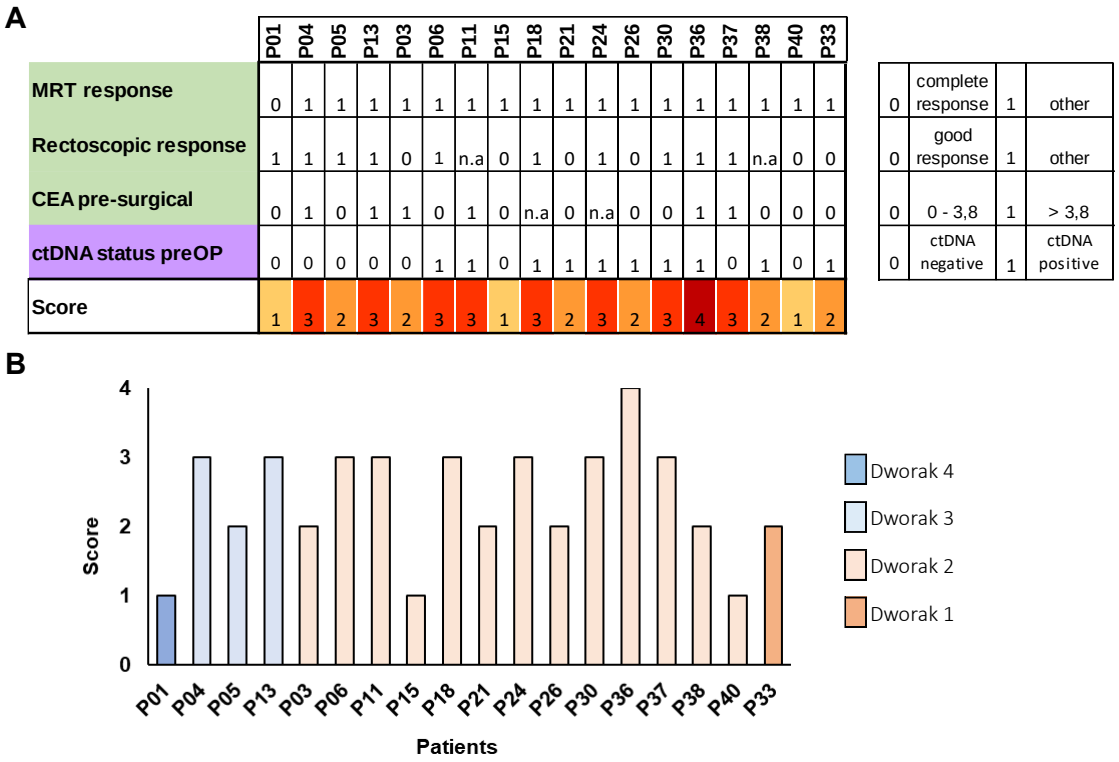

Figure 18: Composite search of clinical modalities and ctDNA before surgery (V4)

A- Forming a pre-surgical scoring based on clinical parameters assessed in the context of clinical routine diagnostics and ctDNA status at V4.(NeoRect Scoring)
CEA: Carcinoembryonic antigen; n.a.: not assessable / not available; preOP: before surgery

B- NeoRect scoring of individual participants. Coloring dependent on pathologically classified Dworak scoring after surgery from Dworak 4 to 1.

Evaluation of MRI resulted in only one patient showing a complete response to treatment concordant with CEA and ctDNA analysis. Nonetheless, the patient scored one point due to rectoscopic assessment. The other two individuals with only one point appear to have good responses in their rectoscopies and no noticeable CEA and ctDNA values but were described to have a suboptimal response by MRI. Within the six and eight participants with two and 3 points, respectively, the distribution of points varies between the categories. Unfortunately, in two cases rectoscopy was not assessable, and two CEA values were not available. These missing instances were valued as 0 points making an achievement of the highest scoring of 4 impossible. Only one patient summs up to the highest score of 4 points with all modalities depicting bad response to nCRT.

The formed scoring was put in context of the Dworak values defined by the pathologists. The trial participant P01 was classified as a pCR with a Dworak score of 4. Here, our pre-surgical score is also very low (1), solely the rectoscopic assessment wasn´t evaluated as a good response. The other two individuals ranked with only one point were described as Dworak 2. Within the patients with a NeoRect scoring between 2 and 3, the classification of the specimen after TME ranged from Dworak 1 to 3. The worst pathological response as defined by a Dworak score of 1 has a NeoRect scoring of only 2 points, as CEA levels and rectocopic assessment showed good response to therapy. Interestingly, the patient described to have a bad response to therapy in all analyzed parameters was classified as Dworak 2. Overall, no specific pattern can be observed between the formed NeoRect scoring based on presurgical parameters and pathologically categorized Dworak scores after TME.

To further underpin the independency of presurgical parameters and evaluate their impact on predicting tumor response to therapy, clustering of MRI, rectoscopy, CEA value and ctDNA evaluation was conducted as pictured in Figure 19.

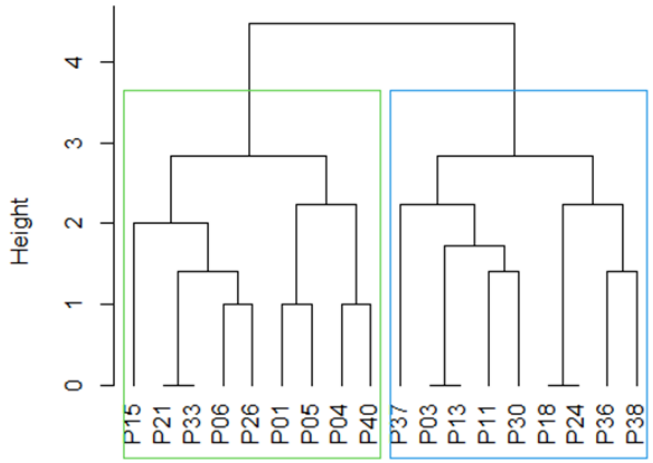

Figure 19: Clustering of the 18 patients with complete serial data available based on presurgical clinical parameters and ctDNA evaluation before TME (V4)

Presurgical clinical parameters included are MRI, rectoscopy and CEA values. MRI and rectoscopy were categorized as good or no response to therapy, CEA values as physiological (0-3,8 ng/ml) or elevated and ctDNA positive or negative.
Cluster was split in two main groups based on two possible outcomes after therapy (pCR/SR vs. no pCR).

The analysis results in two distinctive clusters. Both individuals with pCR/SR (P01 and P04) can be found closely related within the same group. Participant P05, who was also classified with a favorable Dworak score of 3, can also be observed in the same branch.

Nevertheless, P13 is categorized in the opposite group despite the same Dworak scoring as P04 and P05. Instead, P40 clusters closely although classified as Dworak 2. But, interestingly, these four patients (P01, P04, P05 and P40) share the same ctDNA group (ctDNA not detectable at any timepoint). The worst Dworak score of 1 was described once in P33. Clustering based on presurgical parameters ranks this case between specimens reported as Dworak 2 and even in the same group as the patients with a pCR and SR. Taken together, the clustering of parameters assessed before surgery follow no specific pattern and validate that these values taken together are not suffice to distinguish between the observed outcome as defined by the Dworak score after TME and therefor to predict therapy response before TME.

3.2.6. ctDNA dynamics in a setting of metastatic recurrence

As described above blood samples of participants in this trial were taken at three timepoints during nCRT (V1-V3) and once before resection of the primary tumor (V4). In one case (P06) clinical assessment before TME showed an appearance of new metastases in the liver. For this reason, the patient underwent surgery of the liver first and TME of the primary tumor five weeks afterwards. Therefore, we extended the LBx

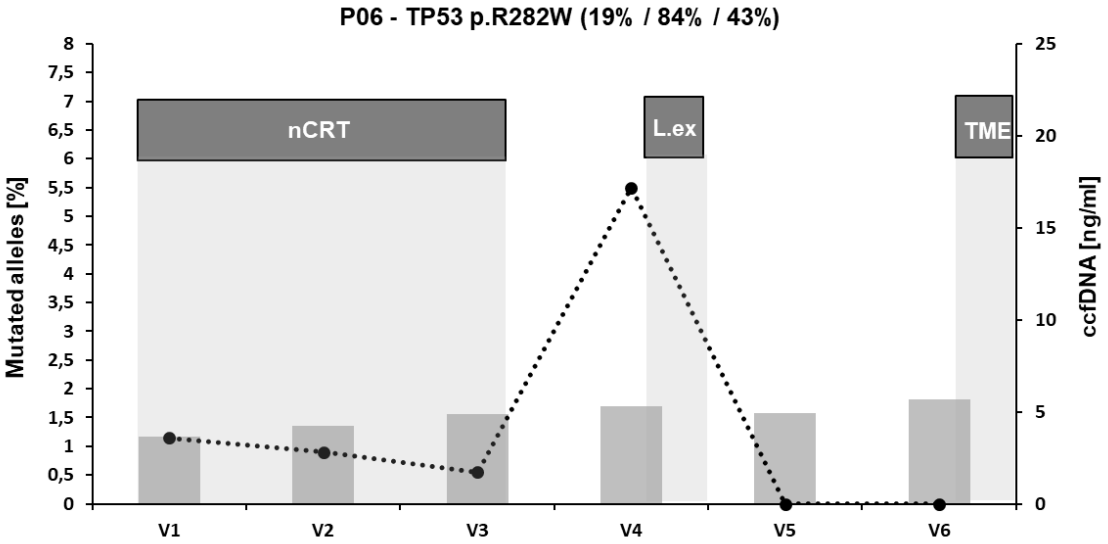

Figure 20: Dynamics of LBx (ct and cfDNA) in a patient with metastatic recurrence during nCRT and a liver first approach

CtDNA ist described as percentage of mutated alleles within the analyzed dPCR (dotted line) and cfDNA as ng per milliliters plasma (grey bars). The headline describes the patient ID, its mutated gene and hotspot traced by dPCR as well as the VAFs detected by NGS in the respective tissue in brackets (primary tissue / liver metastasis / resected specimen).
nCRT: neoadjuvant chemoradio therapy, L. ex: excision of liver metastases; TME: total mesorectal excision;

analysis over two more samplings (V5 and V6) until the date of resection of primary tumor (Figure 20).

At the time of diagnosis, a mutation in the TP53 hotspot was detected by NGS in this patient with 19% mutated alleles within the microdissected area. This aberration was used to track ctDNA in the dPCR.

CtDNA was constantly detectable during nCRT (V1 – V3) and showed a slight decrement from 1,15% to 0,55% mutated alleles. A day before the planed TME, the blood draw defined as V4 was obtained and depicted a ten-fold increment of ctDNA (5,5% mutated alleles). Therefore, patient P06 was categorized into the group of ctDNA increment and the presurgical evaluations at this timepoint were taken into consideration for the described multimodal analysis above. However, as the treating physicians decided to follow the “liver first”-protocol, the primary tumor was not resected yet and the participant was further observed in the context of the trial. Sequencing of the resected liver metastasis showed a VAFs of 84% of the initially detected TP53 mutation, suggesting the metastasis arose from a clone harboring this genetical aberration. To further track ctDNA dynamics, an additional sample was obtained two weeks after liver surgery (V5). At this time point, a complete ctDNA clearance was observed for the first time. CtDNA remained negative until the day before TME (V6). Final sequencing of the primary tumor after resection yields a VAFs of 43% and the individual was pathologically classified as no pCR with a Dworak score of 2. CfDNA quantity showed no great variances throughout all analyzed time points (3,6 – 5,3 ng/ ml plasma).

3.2.7. Association of ctDNA analysis and disease-free survival

Independently of the strength of presurgical parameters and ctDNA to predict tumors´ pathological remission status before TME, analysis of their impact on disease-free survival (DFS) was conducted. (Figure 21)

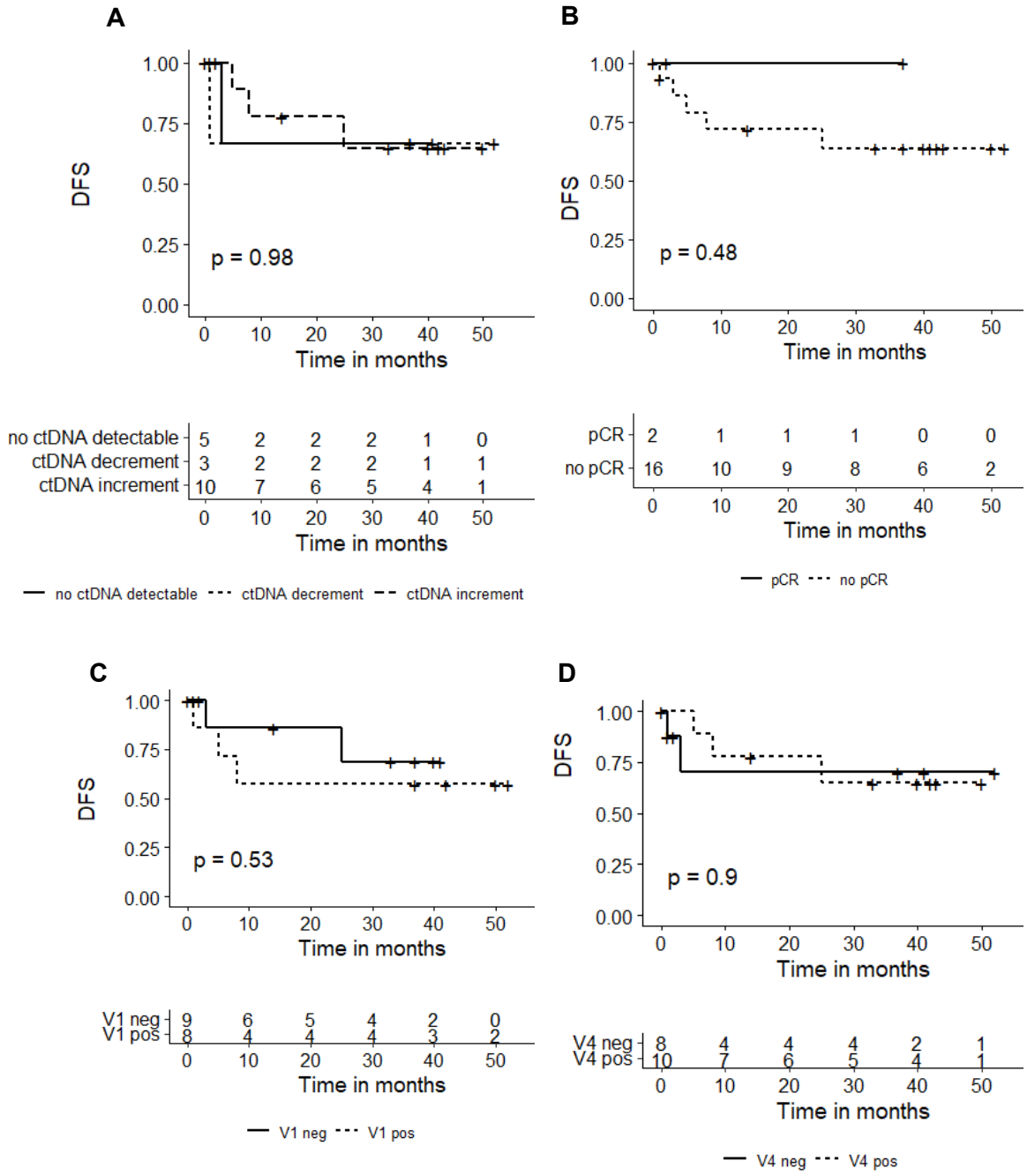

Figure 21: Visual representation of the disease-free survival function over time depending on detected events at the last time of contact

Grouped by (A) ctDNA dynamics, (B) pathological remission status, (C) depending on V1 ctDNA (even distribution) and (D) depending on V4 ctDNA .
Endpoint was defined as time of last contact. Statistical significance was tested based on the log-rank method. P-Values under 0,05 are defined as statistically significant.

DFS was described as no recurrence of primary tumor or distant metastases. The time of last contact of the trial participants varied between one and fifty-two months after surgery. Seventy-two percent stayed disease free during this time. Within the five individuals with an evident disease progression three were categorized in the group of ctDNA increment, one had no ctDNA detectable and one was observed to have a decrement in ctDNA dynamics. The individuals with decremental ctDNA values was the only recorded to have passed away. The biggest discrepancy of the three groups is after 10 months – at this time patients with a described incremental ctDNA dynamic are over 75% likely to maintain a DFS compared to both other groups (Figure 17 A). This curve drops to the same values as the group of not detectable and decremental ctDNA after 25 months. Nevertheless, based on the data available for the 18 participants with complete data sets, our three defined ctDNA groups depict no significantly different distribution curves (log-rank p-value= 0.98).

As ctDNA dynamics have no effect on the DFS, single ctDNA timepoints were examined. CtDNA detection before surgery (V4) shows no significant distribution curves similar to the results of the dynamic grouping (Figure 17 D). Interestingly, LBx analysis before the start of nCRT (baseline/ V1), although not statistically significant, allows the best discrimination between the groups (log-rank p-value= 0.5) (Figure 17 C). These results suggest that DFS might be connected to fundamental differences underlay from the beginning of the disease rather than to its development during and reaction to therapy.

To compare the impact of ctDNA analysis to the standards of routine diagnostics, we conducted the same analysis with the pathological remission status recorded after TME (Figure 17 B). Here, the diseased patient was described to show no pCR after surgery. The two participants with pCR after pathological examination (P01 and P04 SR), remained disease free over the time observed. However, over 68% of the patients recorded to show no pCR also appear as disease-free. Following this categorization, the p-value is lower than separated by ctDNA dynamics, but the differences are still not statistically significant (log-rank p-value= 0.48).

4. Discussion

In the past decades great advances have been made in treatment of RC.[15] In fact, the implementation of a combined chemo- and radiotherapy before surgery has led to 30% of patients showing a pathological CR after treatment.[14] Although W&W approaches have shown to perform greatly within this population, there is an unmet need of predictive factors to detect these individuals reliably before TME.[26] Liquid biopsy is a novel minimal invasive approach that enables analysis of different aspects of diseases and has been used in the context of cancer for early cancer detection and as a MRD marker among others.[53]

Here, we used a targeted LBx approach to investigate the predictive role of ctDNA in patients with locally advanced RC in the NeoRect trial. Beforehand we established a LBx protocol providing a basis for a routinely applicable technique for the University hospital of Augsburg.

4.1. Analytical foundation of ctDNA analysis in the clinic

4.1.1. Plasma volume and cfDNA isolation

Blood samples are collected for several analysis in the clinical routine such as blood counts, clinical chemistry (e.g. organ values or enzymes) and tumor markers such as CEA values in the context of cancer. LBx can be obtained in parallel without the need of an additional blood draw. Its minimal invasive character is one of the main advantages compared to tissue biopsies specially when repeated sampling is aimed. Based on the assumption that free DNA is equally distributed throughout the blood circulation, we tested the cfDNA yields depending on the plasma input volume.

A positive correlation can be observed between plasma input and cfDNA quantity- the higher the input volume the more free DNA can be isolated. This effect is independent of the used protocol for DNA isolation. Considering a 9 ml blood draw feasible in the routine, enough analyzable DNA copies per microliter can be obtained from 4 ml plasma without overloading the following reaction in the dPCR chip.

However, it is important to underline that the material used for our analysis was obtained from different individuals. Amount and heritage of cfDNA can be influenced by various variables such as age, disease, physical activity, stress and medication resulting in high variances as observed in our results [69]. This effect has also to be taken into

consideration when routinely working with LBx, as higher numbers of wild-type alleles lead to a dilution of mutated ctDNA of interest and has therefore direct consequences on the LoD of further analysis methods.
Another crucial aspect is DNA integrity. This is of special significance when following examination includes an amplification step as it is e.g. for NGS. In terms of cfDNA, good quality means fragment distribution near 172 bp. This length is characteristic for circulating nucleic acids as it corresponds to nucleosome-bound DNA which is therefore protected from degradation and can give information about nucleosomal occupancy of genes and gene activity [50, 70]. We were able to depict this fragment length using both isolation protocols. However, we observed small fractions of higher molecular DNA after the Qiagen protocol corresponding to oligo-nucleosomal (particularly di-nucleosomal) DNA. This observation has been reported previously in literature [71]. Although not described yet, these molecules´ length and weight difference may influence the following dPCR assay where the reaction space is highly restricted.

As we aimed to establish a successful LBx protocol not only for our NeoRect trial, but also for a possible future use in the routine, there are further important variables to consider besides quantity and quality such as feasibility, complexity, and hands-on time of the future protocol. Pérez-Barrios and colleagues compared three methods of cfDNA isolation including the Promega protocol and a comparable isolation kit from Qiagen. Similar to our results, they also described both methods to be equally efficient in terms of cfDNA yield but the Promega kit being simpler and more rapid [71]. Furthermore, as the minimally invasive nature of the sampling makes longitudinal monitoring feasible, this semi-automated protocol enables managing of higher sample numbers.
In general, there are also other methods for cfDNA isolation. Nonetheless, the Promega system based on magnetic isolation offers a variety of protocols for many other nucleic acids, some of which are already well established and routinely used at the University clinics of Augsburg. Therefore, taking these facts into consideration, we decided to use a LBx protocol with a starting volume of 4ml plasma using the Promega isolation kit for the NeoRect trial.

4.1.2. Using dPCR for a targeted approach

As described above, material from LBx can be analyzed on different levels using a variety of techniques one of them being dPCR for mutation detection. In this context, Bartels and colleagues compared dPCR with two other molecular methods for mutation

detection of the p.T790M resistance mutation in cfDNA from lung cancer patients in routine laboratory practice [72]. They concluded that NGS and dPCR analysis both provide a reliable sensitivity of 0.1% (making them superior to qPCR). This matches the LoD set in the framework of this thesis. Furthermore, they suggest NGS analysis to be the method of choice when finding of primary mutations is needed but dPCR being optimal to track known mutations e.g. in the context of resistance mechanisms in subclones under therapy [72].

Hence, several studies can be found using dPCR (or ddPCR) for ctDNA identification in the context of cancer. Alike Bartels, Riediger and colleagues tracked the *EGFR* resistance mutation in ctDNA of NSCLC patients using dPCR. They compared mutant DNA levels with the course of response to therapy. Herein, they detected between 0,033 and 0,1% mutant alleles allowing conclusion about controlled disease and tumor progression earlier than other current available methods [65]. Furthermore, a prospective clinical trial in 2019 explored both CTC and ctDNA (using ddPCR) in metastatic RC. Here the investigators described persistently detectable ctDNA before surgery of liver metastases to be associated with short post-surgical OS. But although CTC analysis correlated with ctDNA levels, only few patients showed persistently elevated counts during therapy suggesting the need for more sensitive CTC detection techniques and resulting in a superiority of ddPCR analysis [60]. Additionally, several studies have reported individuals with detectable mutation levels in blood by ddPCR analysis while being seemingly wildtype by tumor sequencing indicating sampling at a tumor site without mutation and emphasizing the advantage of ddPCR regarding the overview of tumor heterogeneity [60, 73].

Despite the same functional background, discordances have been reported between the liquid PCR form in droplets (ddPCR) and the solid form (dPCR) for mutation analysis in lung and RC patients. The data shows that dPCR has a higher sensitivity and allows therefore ctDNA detection even in patients with low cfDNA abundance making this specific method an excellent tool for our NeoRect trial [74].

Taken all together, our established protocol consists of cfDNA isolation with the Promega protocol from 4 ml plasma that can habitually be obtained from a 9 ml blood draw. In the context of our NeoRect trial, cfDNA is further analyzed using a targeted approach by dPCR based on a LoD of 0.1%. Nevertheless, on principle, a variety of applications are conceivable for future projects such as sequencing or detection of epigenetic features [70, 75].

4.2. The NeoRect trial

4.3.1 Liquid Biopsy in the context of the Sauer-protocol for locally advanced rectal cancer

The aim of our trial was to examine the power of LBx for outcome prediction in a preoperative setting under nCRT for identification of patients eligible for a W&W approach in the context of RC. Thus, we conducted analysis of ctDNA during neoadjuvant treatment based on a personalized approach using dPCR in non-metastasized RC patients.

The forty participants underwent the so-called Sauer protocol consisting of a combinational therapy of chemo- and radiotherapy before surgery. Despite the relatively low number of individuals in our study, our cohort shows key features of patients with RC as described in literature. Firstly, a proportion of patients are described to respond particularly well to therapy and therefore being potentially eligible for a W&W approach without surgery [14]. In our cohort, the rate of pathologically observed complete remissions amounts to 14% and is therefore slightly lower to the described 20% to 30%. The twelve patients with missing information from external surgeries could compensate the remaining discrepancy. Secondly, the mutational landscape of our investigated cohort is highly comparable. Here, the most frequently detected mutation in the tissue biopsies´ sequencing analysis was at the *TP53* gene. Mutations in this tumor suppressor gene has been shown to affect growth behavior leading to an advantage towards tumor progression and has been reported in many cancer types including RC [6]. The second most frequent alteration was at the *KRAS* gene with 32 %. This is consistent with the expected 40% *KRAS*-positive rectal tumors [8]. Summarizing, our included trial participants reflect the average RC patients nicely therefore making our trial a great foundation for LBx analysis in this disease.

As described above, cell-free DNA can be found circulating in every person. However, patients with RC depict significantly higher cfDNA values than healthy individuals [73]. In this context, several studies have examined cfDNA dynamics in RC. Yet, different treatment variations were included into analysis rather than only focusing on nCRT or cfDNA measurements were evaluated strictly perioperatively instead of during treatment [76]. In breast cancer, for instance, it has been shown that cfDNA can be measured under the influence of neoadjuvant chemotherapy [63]. Furthermore, many have focused on a metastasized stadium, describing cfDNA being detectable in all patients with

metastatic RC [60, 61, 77]. Still, the question remains open, how cfDNA dynamics behave in a clinical setting for patients with advanced RC without metastases going through the Sauer protocol. Our findings suggest, that although not-metastasized, still all individuals suffering from RC depict cfDNA under treatment.

Moreover, in cancer patients a small proportion of cfDNA originates from tumor cells. This ctDNA is described to be released by tumors shedding their genetic material into the bloodstream through e.g. necrosis and apoptosis [45]. It is therefore questionable if ctDNA is also detectable without extrinsic factors knowingly causing cell death such as radiation. However, we were able to detect ctDNA before starting nCRT (V1, baseline) in over 60% of the participants. As we included locally advanced tumors, this ctDNA may originate from foci of necrotic or apoptotic cell death (and potentially even from mitosis) which are described to occur spontaneously in advanced solid malignancies [78]. Anyway, although only patients with an advanced disease included, ctDNA positivity differs at baseline suggesting other factors to have an influence. TNM classification, for instance, has been shown to influence ctDNA quantity. Bettegowda and colleagues described a direct correlation between ctDNA and tumor stage in RC [52]. Furthermore, because LBx depicts an image of general tumor burden, ctDNA quantity in RC could be influenced by lymph node positivity as it does for breast cancer [79]**.** Also, artificially increased cfDNA due to factors such as comorbidity, infections, smoking, etc. can lead to wrong negative ctDNA results. Interestingly, both patients with pCR/SR had negative ctDNA results before treatment initiation, which is especially remarkable, as only one third of the individuals had a negative ctDNA status at baseline. This fits the fact that necrotic advanced tumors are often associated with poor prognosis [78] and therefore ctDNA-negative individuals at baseline are expected to have greater outcomes .

By the end of therapy (V3) ctDNA could be detected in only a small proportion of patients. This reflects the expected shrinkage of tumor size resulting in lower DNA being released. This dynamic was previously described not only for ctDNA but also for CTCs in the context of RC [60]. However, at this timepoint we observed ctDNA negativity in both, good as well as bad responders. This was also the case one day before surgery (V4). As there are several treatment-free weeks before TME, ctDNA at this timepoint is of special interest. Here, over 50% showed ctDNA positivity which can be interpreted as an “active” tumor. Consequently, all these individuals had residual tumoral mass after TME. The observed correlation between V4 ctDNA status and postsurgical Dworak scores was statistically confirmed in our trial. However, not all ctDNA-negative patients at V4 reached a pathological complete remission status. This poor correlation was previously described

by Tie and Cohen and colleagues in a study of 2019. Here, they also concluded that ctDNA analysis within a short interval following neoadjuvant therapy cannot discriminate patients eligible for a non-operative approach [80].

Nevertheless, presurgical LBx analysis stood out in one participant, as it was ten times higher than at the end of therapy. This patient had suffered from new metastases in the absence of therapy. Sequencing results revealed that the new liver metastasis arose from cells harboring the tracked mutant allele. This case emphasizes the role of ctDNA depicting patient´s overall tumor burden.

However, taken together, ctDNA analysis at any single timepoint of our trial design appears to not give enough information for response prediction which is consistent with findings in previous studies [76, 80].

Consequently, looking at ctDNA dynamics may be more promising. As mentioned before, the goal of a neoadjuvant combinational therapy before surgery is to shrink the primary tumor and to reduce and limit tumor spread to other organs. Therefore, significant decrement of the ctDNA detection rate during nCRT is presumably due to tumor shrinkage reducing the available ctDNA quantity. In a study of 2020, Murahashi and colleagues described two groups of ctDNA dynamics during preoperative therapy of locally advanced rectal cancer. They examined ctDNA at baseline and after preoperative treatment defined as before surgery (analogous to our V4). They found a significant association between response to therapy and ctDNA changes, as good responders showed decremental and non-responders incremental ctDNA dynamics, respectively [76]. This is comparable to the classification defined in our study. Nonetheless, although we described similar grouping, we were not able to distinguish patients´ response to therapy. Though, we included a third group with no ctDNA detectable at any timepoint. Remarkably, patients with great response to therapy (pCR and SR) were classified in this group. Although Murahashi and colleagues described good responders to have a decreasing ctDNA dynamic, they only included individuals with positive ctDNA results in at least one measurement into their cohort hence omitting cases with constant negative results [76]. However, there were also other individuals within this group but without pCR. One of those was tracked by a mutation found at an extremely low VAF in the resected specimen. Here, missing ctDNA: can be a result of either, the mutation evolving during therapy and therefore being absent during previous measurements or the subclone harboring this mutation being underrepresented at the beginning and not being detected with our method´s sensitivity. But still, missing ctDNA at all timepoints is not an exclusive feature of good responders. This observation coincides with the results from Carpinetti

and colleagues, who described negative ctDNA levels in a patient with pCR but, unfortunately, also in patients presenting incomplete response even with significant tumor regression [81].

In summary, LBx analysis is possible in a neoadjuvant setting for locally advanced RC Our experiments show that no ctDNA can be detected in patients with great response to therapy. Although this characteristic is not unique for these individuals, increased ctDNA levels, specially before TME, indicate remaining tumor mass or even metastatic tumor spread.

4.3.2 Prognostic value of liquid biopsy incorporating multimodal aspects and disease-free survival

Analysis of LBx in RC patients seems to give a hint about the tumor´s response to therapy but is not suffice to reliably discriminate great responders for a W&W approach. Therefore, we hypothesized that incorporating ctDNA into a scoring system with other routinely obtained modalities might show a cumulative impact.

Previous studies have already examined LBx analysis combined with other modalities. The most conventional tumor marker for RC patients for therapeutic efficacy is the CEA value. This antigen is an intracellular protein which is not only normally found in low concentrations in embryonic gut but is also expressed in normal adult tissues and has been described to provide a variety of cellular functions in cancer supporting tumor invasion and metastasis.[82] The distinct biological characteristics compared to (ct)DNA is a potential reason for the independency of the parameters as no correlation was reported in our study. In a study of 2021, Osumi et al. evaluated the relationship between plasma CEA values and ctDNA levels in 110 individuals with RC. Similarly, they reported a low correlation between ctDNA and CEA status in patients without liver metastasis. Furthermore, they described both parameters to be affected by tumor volume with an increased number of false negative results in smaller tumor cases.[83] This effect has to be also considered in our study design, as analysis were conducted after nCRT which leads to tumor shrinkage in most cases. Nonetheless, interestingly, presurgical CEA values of P06, who showed to have new liver metastases before planned TME and a 10-fold ctDNA increment, were within the physiological range. In this case, there is an extensive discrepancy between both variables with LBx drawing a more precise picture of the reality of the disease status.

Another study of 2020 also aimed to predict pathological response of RC after preoperative therapy using ctDNA. Here, ctDNA data was described to have positive predictive values when combined with endoscopic findings suggesting combinational analysis of LBx with clinical factors.[76] However, rectoscopy results are not always available, as e.g. experts reported two cases as “not assessable” within our NeoRect trial. Likewise, Wang and colleagues explored the value of ctDNA in combination with MRI in the prediction of pCR before surgery. They also described an improvement of the predictive performance in a model with LBx supplementing MRI compared to the individual information. [84]
Taken together, there is wide evidence of ctDNA improving predictive models combined with single modalities. For this reason, we built a scoring system consisting of all four parameters: CEA levels, MRI and rectoscopic response and ctDNA values before TME. To do so, we distributed points for every description other than physiological (for CEA values), good response (for MRI and rectoscopy) or negative (for ctDNA). The less modalities reported bad treatment outcomes the lower the score and, presumably, the better the pathological remission status after TME. However, this proposal could not be validated for the cohort of this thesis. Even though the individual with a Dworak score of 4 (total pCR) was assigned only one point, no further patterns could be observed. For example, a patient with the worst treatment response pathologically described to be Dworak 1 achieved two points in our multimodal scoring system while two cases with a Dworak 3 status showed higher scorings with three points. This observation is confirmed when the presurgical modalities are hierarchically clustered. Although trends are recognizable (e.g. patients with pCR and SR clustering closely) it is not possible to reliably discriminate between patients with good or bad responses to nCRT.

As described above, the results of a previous clinical trial indicate that patients following a W&W approach after nCRT show excellent outcomes after CR without TME with a DFS of 86%.[17] Due to this conclusion we further examined the DFS at the last time of contact based on different ctDNA timepoints assuming that distinct ctDNA dynamics portray superior therapy response, and therefore longer DFS, in individuals that could have been eligible for a conservative treatment option. However, this hypothesis could not be validated in this cohort. Neither ctDNA dynamics grouped as described above nor baseline ctDNA before nCRT or directly before surgery as single timepoints are significant predictors for greater DFS. Nevertheless, it is crucial to highlight that, according to literature, individuals with pCR after TME are expected to show significantly

longer DFS and OS.[85] This could also not be confirmed in the two individuals with pCR of the NeoRect trial which makes the representativeness of the explored cohort questionable. And although literature suggests comparable outcomes, W&W approaches pose danger of hidden residual tumor cells capable of reactivating the disease. In this context previous studies have shown the power of postsurgical ctDNA as a marker for MRD and a predictor on the rate of recurrence-free survival.[67, 76, 86] Therefore, investigation of ctDNA after TME rather than before appears to be the more precise tool for DFS analysis.

In conclusion, our study suggests that the NeoRect trail provides an excellent platform to investigate how personalized ctDNA monitoring can complement imaging and clinical evaluation of tumor response. Although the examined effects are insufficient to prevent TME in RC patients, many interesting observations were made that should be further explored in future projects with bigger cohorts.

4.3.3 Strengths and limitations of our study

Several features of our study design stand out specifically. To begin with, we used sequencing data from primary tumor. This procedure is not only the gold standard in the routine but has also other great advantages. For instance, sequencing directly from LBx challenges the possibility to distinguish alterations from clonally expanded hematopoietic stem cells caused by leukemogenic mutations. These so-called CHIPs (clonal hematopoiesis of indeterminate potential) are an age-related phenomenon, and an increased prevalence is associated with heritable as well as acquired risk factors such as unhealthy lifestyle and cancer therapy among others. It describes the presence of clonally expanded hematopoietic cells without evidence of a malignancy in blood [87]. Hence, discriminating these events for ctDNA analysis is crucial.
Subsequent we conducted a personalized approach by targeting the respective mutation using dPCR. As described above, a main advantage of this method is its high sensitivity. But there are also other great benefits: The low costs per sample make longitudinal studies with multiple samplings feasible. Furthermore, hands-on time in the laboratory is short and results can be obtained quickly within around three hours (in comparison NGS library preparation takes about 3 days). On top of that, data analysis afterwards is straightforward and needs only few bioinformatics making this method again faster and easier.

Next, we aimed for a multimodal concept in the NeoRect trial. Numerous studies have explored the correlation between ctDNA and clinical factors [76, 88]. However, we incorporated all clinical parameters routinely obtained before TME in order to draw the best overall picture of tumor response, hypothesizing ctDNA to complement sensibly and therefor be able to identify individuals with pCR. To our knowledge this is the first study including all these variables advocating for a multimodal scoring system.
Finally, we incorporated analysis of DFS. Although this was not a focus of this thesis, many studies before indicated a correlation between LBx and follow-up results making it an interesting question.

Nonetheless, there are also several limitations. First, unfortunately the number of recruited patients assessed was small with a high drop-out rate. On the one hand, several patients had surgery at external institutions which led to missing both presurgical blood draw and staging and the postsurgical pathological remission status disallowing correlation analysis. A multicenter study would help to significantly increase the number of participants but comes with several organizational obstacles such as samples and information flow specially regarding the interdisciplinary aspect within each institution. On the other hand, numerous individuals had either no trackable mutation in the sequenced tissue biopsy nor an according dPCR assay available for the detected mutation. This limited the possibility to track ctDNA in these participants using dPCR. Although assays could potentially be designed for each mutation, it is high in costs.
Moreover, we included only patients undergoing a neoadjuvant chemoradiation following the Sauer-protocol. Other therapy options, such as TNT, and possible dosing variations were omitted and should be taken into consideration in a larger cohort.
As described above, a targeted approach as we chose for this trial has several benefits. However, the missing of potential relevant clones is a significant disadvantage as targeting only one clonal marker neglects information about inter- and intratumoral heterogeneity. Therefore, metastases from subclones harboring a different mutation would falsely have no impact on the ctDNA analysis of this study. Furthermore, it is also not possible to image longitudinal tumor evolution losing potentially relevant information about the tumors´ response to treatment which can lead to resistance mechanisms and worst outcome.
Lastly, although many modalities were included into our study, many thinkable confounding factors such as gender, distance from anal verge, tumor size and

comorbidities were omitted in the analysis. Further research is needed with a higher patient number to incorporate and statistically evaluate these parameters additionally.

4.3. Future perspectives

About twenty thousand new rectal cancers are diagnosed yearly in Germany. Fortunately, the mortality rate has decreased drastically due early detection and novel and sophisticated therapy options. A combination of chemo- and radiotherapy limits and shrinks the tumor prior to surgery for better outcomes. But surgical procedures are often followed by different complications. Given the fact that 30% of neoadjuvant treated patients might not profit from surgery, reliable identification of these individuals is crucial. Thus, established diagnostic tools such as MRI and rectoscopic evaluation allow insufficient information. LBx has the potential to improve the prognostic value of already existing tools.

With the NeoRect trial described in this thesis a proof of concept was established which enables analysis of tumor derived DNA during therapy of locally advanced rectal cancer. In this study, we focused solely on analysis before surgery. However, postsurgical monitoring of ctDNA during adjuvant follow-up has the potential of early detection of residual disease and recurrence prediction; aspects of central importance concerning potential W&W approaches without surgery after nCRT. A future study with a noticeably bigger cohort should include both, LBx analysis during treatment and after surgery.

Furthermore, the establishment of this analytical method at the university hospital of Augsburg offers the opportunity to use LBx in many different contexts, not only for research purposes but also for routine diagnostics. For instance, LBx analysis of the p.T790M resistance mutation, as used for LoDo analysis in this thesis, can be applied on NSCLC patients. But also, further utilization for a variety of genetic alterations and different cancer types is conceivable. In addition, other body fluids, such as cerebrospinal fluid, and other DNA modifications, such as epigenetic methylation patterns, can be analyzed following the cfDNA isolation protocol established in this thesis.

Finally, there are already ongoing studies integrating ctDNA testing of many cancer-related genes in parallel based on NGS technology. In the future, large amounts of clinical data should be included to improve patient selection and management.

Summary

Locally advanced rectal cancer (RC) is treated with neoadjuvant chemoradiotherapy (nCRT) followed by total mesorectal excision (TME). Under this regime, complete pathologic remissions (pCR) can be observed in about 30% of the patients making the need of a surgical intervention questionable. For this reason, several studies and case series compared this strategy with a “watch and wait” (W&W) approach and reported similar excellent outcomes. Thus, non-surgical treatment for locally advanced RC might constitute a treatment option for selected patients. However, there is an unmet need for reliable biomarkers predicting pCR. The analysis of circulating tumor DNA (ctDNA) has been shown to be suitable for monitoring treatment response and detecting minimal residual disease (MRD). In the context of patients with RC undergoing nCRT, we hypothesized that monitoring ctDNA changes might facilitate identifying individuals reaching pCR and thereby prospectively guiding therapy.

Following the established protocol beforehand, we conducted a prospective single center study with forty RC patients subjected to nCRT and TME (NeoRect trial). Plasma samples were collected before, during and after nCRT and before TME. Circulating free DNA was extracted from 4 ml plasma. Informative somatic mutations were identified initially in biopsies by NGS and subsequently used for ctDNA quantification by a targeted dPCR approach. In over 60% of the participants ctDNA was detectable before starting nCRT and three different dynamics can be observed during treatment (ctDNA increment, decrement and no ctDNA). For instance, good responders to therapy have no detectable ctDNA at any timepoint. Furthermore, a ten-fold ctDNA increment in one patient reflected its newly appeared metastases after therapy distinctively. However, the results show low specificity as no significant association of ctDNA and response can be described. A multimodal approach adding routinely obtained parameters (MRT, rectoscopy and CEA values) is still insufficient to reliable discriminate patients with excellent outcomes before TME. Also, no prognostic association was observed neither with ctDNA dynamics nor single timepoints.

In summary, the NeoRect trial proofs the feasibility of a ctDNA-based personalized monitoring of RC patients under nCRT. The potential of this method to fine-tune the prediction of pCR for a W&W approach needs to be investigated further in bigger cohorts integrating analysis of many cancer genes in parallel and including larger amounts of clinical data.

Zusammenfassung

Lokal fortgeschrittene Rektumkarzinome werden mit neoadjuvanter Chemoradiotherapie (nCRT) und anschließender totaler mesorektaler Exzision (TME) behandelt. Dabei werden bei 20-30 % der Patienten vollständige pathologische Remissionen (pCR) beobachtet. Mehrere Arbeiten, in denen die TME einer "Watch and Wait"-Strategie (W&W) gegenübergestellt wurde, beschreiben vergleichbar gute Ergebnisse. Somit könnte ein nicht-chirurgischer Ansatz eine Behandlungsoption für ausgewählte Patienten darstellen. Es fehlen jedoch zuverlässige Biomarker, die eine pCR vorhersagen. Zirkulierende Tumor-DNA (ctDNA) eignet sich zur Überwachung des Therapieansprechens und zum Nachweis minimaler Resterkrankungen. Daher stellen wir die Hypothese, dass die Überwachung von ctDNA bei Patienten mit RC die Identifizierung von Personen, die eine pCR erreichen, ermöglicht und somit die Therapie prospektiv steuern könnte. Einem zuvor festgelegten Protokoll folgend, führten wir eine prospektive Studie mit vierzig RC-Patienten durch (NeoRect-Studie). Plasmaproben wurden vor, während und nach nCRT und vor der TME entnommen. Freie DNA wurde aus 4 ml Plasma extrahiert. Informative Mutationen wurden in Biopsien durch NGS identifiziert und anschließend zur ctDNA-Quantifizierung durch einen gezielten dPCR-Ansatz verwendet. Bei über 60 % der Teilnehmer war ctDNA vor Beginn der nCRT nachweisbar. Während der Behandlung lassen sich drei verschiedene Dynamiken beobachten (Anstieg der ctDNA, Rückgang und keine ctDNA). So ist bei denjenigen, die gut auf die Therapie ansprechen, zu keinem Zeitpunkt ctDNA messbar. Darüber hinaus spiegelte in einem Fall ein 10-facher ctDNA-Anstieg neu aufgetretene Metastasen nach nCRT deutlich wider. Die Ergebnisse zeigen jedoch eine geringe Spezifität, da kein signifikanter Zusammenhang zwischen ctDNA und Ansprechen beschrieben werden kann. Ein multimodaler Ansatz unter Einbeziehung routinemäßig erhobener Parameter (MRT, Rektoskopie und CEA-Werte), ist ebenfalls unzureichend, um Patienten mit gutem Ansprechen vor TME zuverlässig zu identifizieren. Auch wurde weder bei ctDNA-Dynamik noch bei einzelnen Zeitpunkten ein prognostischer Zusammenhang festgestellt. Zusammenfassend beweist die NeoRect-Studie die Machbarkeit einer auf ctDNA basierenden personalisierten Überwachung von RC-Patienten unter nCRT. Das Potential dieser Methode bei der Feinabstimmung der Vorhersage der pCR für einen W&W-Ansatz muss in größeren Kohorten weiter untersucht werden, indem mehrere Gene parallel analysiert und größere Mengen klinischer Daten einbezogen werden.

References

1. e.V., D.G.f.H.u.M.O., *Onkopedia Leitlinien Kolonkarzinom*. 2022.
2. *S3-Leitlinie Kolorektales Karzinom*. 2019.
3. Katja Anita Oppelt, S.L., Klaus Kraywinkel and Ulrike Haug, *Incidence of advanced colorectal cancer in Germany: comparing claims data and cancer registry data.* BMC Medical Research Methodology, 2019.
4. Cardoso, R., et al., *Incidence and Mortality of Proximal and Distal Colorectal Cancer in Germany-Trends in the Era of Screening Colonoscopy.* Dtsch Arztebl Int, 2021. **118**(16): p. 281-287.
5. DAVID R. RUDY, M.D., M.P.H., AND MICHAEL J. ZDON, M.D., *Update on Colorectal Cancer* Am Fam Physician, 2000.
6. Vogelstein, E.R.F.a.B., *A Genetic Model of Colorectal Tumorgenesis.* Cell, 1990. **61**.
7. Ponz de Leon, M. and A. Percesepe, *Pathogenesis of colorectal cancer.* Dig Liver Dis, 2000. **32**(9): p. 807-21.
8. Dietel, M., et al., *[Molecular pathologic KRAS mutation analysis. A prerequisite of effective antibody treatment for metastasized colorectal cancer].* Chirurg, 2008. **79**(6): p. 576-9.
9. Ralf-Dieter Hofheinz, D.A., Markus Borner, Gunnar Folprecht, B. Michael Ghadimi, Ullrich Graeven, Birgit Grünberger, Holger Hebart, Susanna Hegewisch-Becker, Volker Heinemann, Ron Pritzkuleit, Claus Rödel, Holger Rumpold, Josef Thaler, Tanja Trarbach, Bernhard Wörmann and I.K.m.d. AIO, *Onkopedia Leitlinien Rektumkarzinom*. 2022.
10. Meade, P.G., et al., *Preoperative chemoradiation downstages locally advanced ultrasound-staged rectal cancer.* Am J Surg, 1995. **170**(6): p. 609-12; discussion 612-3.
11. Heald, R.J., *The 'Holy Plane' of rectal surgery.* J R Soc Med, 1988. **81**(9): p. 503-8.
12. Garcia-Aguilar, J., et al., *Organ Preservation in Patients With Rectal Adenocarcinoma Treated With Total Neoadjuvant Therapy.* J Clin Oncol, 2022. **40**(23): p. 2546-2556.
13. e.V., D.G.f.H.u.M.O., *Onkopedia Leitlinien Rektumkarzinom.* 2022.
14. Kong, J.C., et al., *Outcome and Salvage Surgery Following "Watch and Wait" for Rectal Cancer after Neoadjuvant Therapy: A Systematic Review.* Dis Colon Rectum, 2017. **60**(3): p. 335-345.
15. Habr-Gama, A., et al., *Preoperative chemoradiation therapy for low rectal cancer. Impact on downstaging and sphincter-saving operations.* Hepatogastroenterology, 2004. **51**(60): p. 1703-7.
16. Renehan, A.G., et al., *Watch-and-wait approach versus surgical resection after chemoradiotherapy for patients with rectal cancer (the OnCoRe project): a propensity-score matched cohort analysis.* Lancet Oncol, 2016. **17**(2): p. 174-183.
17. Habr-Gama, A., et al., *Operative versus nonoperative treatment for stage 0 distal rectal cancer following chemoradiation therapy: long-term results.* Ann Surg, 2004. **240**(4): p. 711-7; discussion 717-8.

18. Martens, M.H., et al., *Long-term Outcome of an Organ Preservation Program After Neoadjuvant Treatment for Rectal Cancer.* J Natl Cancer Inst, 2016. **108**(12).

19. Smith, R.K., et al., *Surveillance after neoadjuvant therapy in advanced rectal cancer with complete clinical response can have comparable outcomes to total mesorectal excision.* Int J Colorectal Dis, 2015. **30**(6): p. 769-74.

20. Smith, J.J., et al., *Assessment of a Watch-and-Wait Strategy for Rectal Cancer in Patients With a Complete Response After Neoadjuvant Therapy.* JAMA Oncol, 2019. **5**(4): p. e185896.

21. Maas, M., et al., *Wait-and-see policy for clinical complete responders after chemoradiation for rectal cancer.* J Clin Oncol, 2011. **29**(35): p. 4633-40.

22. Habr-Gama, A., et al., *Baseline T Classification Predicts Early Tumor Regrowth After Nonoperative Management in Distal Rectal Cancer After Extended Neoadjuvant Chemoradiation and Initial Complete Clinical Response.* Dis Colon Rectum, 2017. **60**(6): p. 586-594.

23. Habr-Gama, A., et al., *Local recurrence after complete clinical response and watch and wait in rectal cancer after neoadjuvant chemoradiation: impact of salvage therapy on local disease control.* Int J Radiat Oncol Biol Phys, 2014. **88**(4): p. 822-8.

24. van der Valk, M.J.M., et al., *Long-term outcomes of clinical complete responders after neoadjuvant treatment for rectal cancer in the International Watch & Wait Database (IWWD): an international multicentre registry study.* Lancet, 2018. **391**(10139): p. 2537-2545.

25. Simpson, G., et al., *Long-term outcomes of real world 'watch and wait' data for rectal cancer after neoadjuvant chemoradiotherapy.* Colorectal Dis, 2020. **22**(11): p. 1568-1576.

26. Gani, C., A. Kirschniak, and D. Zips, *Watchful Waiting after Radiochemotherapy in Rectal Cancer: When Is It Feasible?* Visc Med, 2019. **35**(2): p. 119-123.

27. Patel, U.B., et al., *MRI assessment and outcomes in patients receiving neoadjuvant chemotherapy only for primary rectal cancer: long-term results from the GEMCAD 0801 trial.* Ann Oncol, 2017. **28**(2): p. 344-353.

28. Bakke, K.M., et al., *Diffusion-weighted magnetic resonance imaging of rectal cancer: tumour volume and perfusion fraction predict chemoradiotherapy response and survival.* Acta Oncol, 2017. **56**(6): p. 813-818.

29. Dayde, D., et al., *Predictive and Prognostic Molecular Biomarkers for Response to Neoadjuvant Chemoradiation in Rectal Cancer.* Int J Mol Sci, 2017. **18**(3).

30. van der Sande, M.E., et al., *Response assessment after (chemo)radiotherapy for rectal cancer: Why are we missing complete responses with MRI and endoscopy?* Eur J Surg Oncol, 2019. **45**(6): p. 1011-1017.

31. Haber, D.A. and V.E. Velculescu, *Blood-based analyses of cancer: circulating tumor cells and circulating tumor DNA.* Cancer Discov, 2014. **4**(6): p. 650-61.

32. Lone, S.N., et al., *Liquid biopsy: a step closer to transform diagnosis, prognosis and future of cancer treatments.* Mol Cancer, 2022. **21**(1): p. 79.

33. de Bono, J.S., et al., *Circulating tumor cells predict survival benefit from treatment in metastatic castration-resistant prostate cancer.* Clin Cancer Res, 2008. **14**(19): p. 6302-9.

34. Cohen, S.J., *Relationship of circulating tumor cells to tumor response, progression-free surival, and overall survival in patients with metastatic colorectal cancer.* J Clin Oncol., 2008.

35. Andree, K.C., G. van Dalum, and L.W. Terstappen, *Challenges in circulating tumor cell detection by the CellSearch system.* Mol Oncol, 2016. **10**(3): p. 395-407.

36. De Angelis, M.L., et al., *An organoid model of colorectal circulating tumor cells with stem cell features, hybrid EMT state and distinctive therapy response profile.* J Exp Clin Cancer Res, 2022. **41**(1): p. 86.

37. Zhang, Y., et al., *Exosomes: biogenesis, biologic function and clinical potential.* Cell Biosci, 2019. **9**: p. 19.

38. Skog, J., *Glioblastoma microvesicles transport RNA and proteins that promote tumour growth and provide diagnostic biomarkers.* Nat Cell Biol. , 2008.

39. Pezzicoli, G., et al., *Large Extracellular Vesicles-A New Frontier of Liquid Biopsy in Oncology.* Int J Mol Sci, 2020. **21**(18).

40. Batrakova, E.V. and M.S. Kim, *Using exosomes, naturally-equipped nanocarriers, for drug delivery.* J Control Release, 2015. **219**: p. 396-405.

41. Umu, S.U., et al., *A comprehensive profile of circulating RNAs in human serum.* RNA Biol, 2018. **15**(2): p. 242-250.

42. Xue, V.W., et al., *Non-invasive Potential Circulating mRNA Markers for Colorectal Adenoma Using Targeted Sequencing.* Sci Rep, 2019. **9**(1): p. 12943.

43. Marilesia Ferreira de Souza, H.K., Mateus de Camargo Barros-Filho, Heloísa Lizotti Cilião, Fabio Albuquerque Marchi, Paulo Emilio Fuganti, Alexandre Rossi Paschoal, Silvia Regina Rogatto, Ilce Mara de Syllos Cólus, *Circulating mRNAs and miRNAs as candidate markers for the diagnosis and prognosis of prostate cancer.* PLoS One, 2017.

44. Tan, E.M., et al., *Deoxybonucleic acid (DNA) and antibodies to DNA in the serum of patients with systemic lupus erythematosus.* J Clin Invest, 1966. **45**(11): p. 1732-40.

45. Antonatos, D., et al., *Cell-free DNA levels as a prognostic marker in acute myocardial infarction.* Ann N Y Acad Sci, 2006. **1075**: p. 278-81.

46. Saukkonen, K., et al., *Cell-free plasma DNA as a predictor of outcome in severe sepsis and septic shock.* Clin Chem, 2008. **54**(6): p. 1000-7.

47. Lo, Y.M., et al., *Presence of fetal DNA in maternal plasma and serum.* Lancet, 1997. **350**(9076): p. 485-7.

48. Glenn E Palomaki, E.M.K., Geralyn M Lambert-Messerlian, James E Haddow, Louis M Neveux, Mathias Ehrich, Dirk van den Boom, Allan T Bombard, Cosmin Deciu, Wayne W Grody, Stanley F Nelson, Jacob A Canick, *DNA sequencing of maternal plasma to detect Down syndrome: an international clinical validation study* Genetics in Medicine, 2011. **13**(11).

49. Esagian, S.M., et al., *Comparison of liquid-based to tissue-based biopsy analysis by targeted next generation sequencing in advanced non-small cell lung cancer: a comprehensive systematic review.* J Cancer Res Clin Oncol, 2020. **146**(8): p. 2051-2066.

50. Fan, H.C., et al., *Analysis of the size distributions of fetal and maternal cell-free DNA by paired-end sequencing.* Clin Chem, 2010. **56**(8): p. 1279-86.

51. Leon, S.A., et al., *Free DNA in the serum of cancer patients and the effect of therapy.* Cancer Res, 1977. **37**(3): p. 646-50.

52. Bettegowda, C., et al., *Detection of circulating tumor DNA in early- and late-stage human malignancies.* Sci Transl Med, 2014. **6**(224): p. 224ra24.

53. Corcoran, R.B. and B.A. Chabner, *Application of Cell-free DNA Analysis to Cancer Treatment.* N Engl J Med, 2018. **379**(18): p. 1754-1765.

54. Roberto, T.M., et al., *Strategies for improving detection of circulating tumor DNA using next generation sequencing.* Cancer Treat Rev, 2023. **119**: p. 102595.

55. Sykes, P.J., et al., *Quantitation of targets for PCR by use of limiting dilution.* Biotechniques, 1992. **13**(3): p. 444-9.

56. Devin Dressman, H.Y., Giovanni Traverso, Kenneth W. Kinzler, and Bert Vogelstein, *Transforming single DNA molecules into fluorescent magnetic particles for detection and enumeration of genetic variations.* PNAS, 2003.

57. Hindson, B.J., et al., *High-throughput droplet digital PCR system for absolute quantitation of DNA copy number.* Anal Chem, 2011. **83**(22): p. 8604-10.

58. Palacin-Aliana, I., et al., *Clinical Utility of Liquid Biopsy-Based Actionable Mutations Detected via ddPCR.* Biomedicines, 2021. **9**(8).

59. Phallen, J., et al., *Direct detection of early-stage cancers using circulating tumor DNA.* Sci Transl Med, 2017. **9**(403).

60. Bidard, F.C., et al., *Circulating Tumor Cells and Circulating Tumor DNA Detection in Potentially Resectable Metastatic Colorectal Cancer: A Prospective Ancillary Study to the Unicancer Prodige-14 Trial.* Cells, 2019. **8**(6).

61. Thierry, A.R., et al., *Clinical validation of the detection of KRAS and BRAF mutations from circulating tumor DNA.* Nat Med, 2014. **20**(4): p. 430-5.

62. Chaudhuri, A.A., et al., *Predicting Radiotherapy Responses and Treatment Outcomes Through Analysis of Circulating Tumor DNA.* Semin Radiat Oncol, 2015. **25**(4): p. 305-12.

63. Li, S., et al., *Circulating Tumor DNA Predicts the Response and Prognosis in Patients With Early Breast Cancer Receiving Neoadjuvant Chemotherapy.* JCO Precis Oncol, 2020. **4**.

64. Zhou, Y., et al., *Serial circulating tumor DNA identification associated with the efficacy and prognosis of neoadjuvant chemotherapy in breast cancer.* Breast Cancer Res Treat, 2021. **188**(3): p. 661-673.

65. Riediger, A.L., et al., *Mutation analysis of circulating plasma DNA to determine response to EGFR tyrosine kinase inhibitor therapy of lung adenocarcinoma patients.* Sci Rep, 2016. **6**: p. 33505.

66. Filipits, M., et al., *Epidermal Growth Factor Receptor T790M Mutation Testing in Non-Small Cell Lung Cancer: An International Collaborative Study to Assess Molecular EGFR T790M Testing in Liquid Biopsy.* Cancers (Basel), 2023. **15**(13).

67. Tie, J., et al., *Circulating tumor DNA analysis detects minimal residual disease and predicts recurrence in patients with stage II colon cancer.* Sci Transl Med, 2016. **8**(346): p. 346ra92.

68. O. Dworak, L.K., A. Hoffmann, *Pathological features of rectal cancer after preoperative radiochemotherapy.* Int J Colorect Dis, 1996. **12**: p. 19-23.

69. Yuwono, N.L., K. Warton, and C.A. Ford, *The influence of biological and lifestyle factors on circulating cell-free DNA in blood plasma.* eLife, 2021.

70. Snyder, M.W., et al., *Cell-free DNA Comprises an In Vivo Nucleosome Footprint that Informs Its Tissues-Of-Origin.* Cell, 2016. **164**(1-2): p. 57-68.

71. Perez-Barrios, C., et al., *Comparison of methods for circulating cell-free DNA isolation using blood from cancer patients: impact on biomarker testing.* Transl Lung Cancer Res, 2016. **5**(6): p. 665-672.

72. Bartels, S., et al., *Molecular Analysis of Circulating Cell-Free DNA from Lung Cancer Patients in Routine Laboratory Practice: A Cross-Platform Comparison of Three Different Molecular Methods for Mutation Detection.* J Mol Diagn, 2017. **19**(5): p. 722-732.

73. Zmrzljak, U.P., et al., *Detection of Somatic Mutations with ddPCR from Liquid Biopsy of Colorectal Cancer Patients.* Genes, 2021. **12**(2): p. 289.

74. Crucitta, S., et al., *Comparison of digital PCR systems for the analysis of liquid biopsy samples of patients affected by lung and colorectal cancer.* Clin Chim Acta, 2023. **541**: p. 117239.

75. Jovelet, C., et al., *Circulating Cell-Free Tumor DNA Analysis of 50 Genes by Next-Generation Sequencing in the Prospective MOSCATO Trial.* Clin Cancer Res, 2016. **22**(12): p. 2960-8.

76. Murahashi, S., et al., *Serial circulating tumour DNA analysis for locally advanced rectal cancer treated with preoperative therapy: prediction of pathological response and postoperative recurrence.* Br J Cancer, 2020. **123**(5): p. 803-810.

77. Lee, S., et al., *Clinical Implication of Liquid Biopsy in Colorectal Cancer Patients Treated with Metastasectomy.* Cancers (Basel), 2021. **13**(9).

78. Liu, Z.G. and D. Jiao, *Necroptosis, tumor necrosis and tumorigenesis.* Cell Stress, 2019. **4**(1): p. 1-8.

79. Zhou, Y., et al., *Clinical factors associated with circulating tumor DNA (ctDNA) in primary breast cancer.* Mol Oncol, 2019. **13**(5): p. 1033-1046.

80. Tie, J., et al., *Serial circulating tumour DNA analysis during multimodality treatment of locally advanced rectal cancer: a prospective biomarker study.* Gut, 2019. **68**(4): p. 663-671.

81. Carpinetti, P., et al., *The use of personalized biomarkers and liquid biopsies to monitor treatment response and disease recurrence in locally advanced rectal cancer after neoadjuvant chemoradiation.* Oncotarget, 2015. **6**(35): p. 38360-71.

82. In Ja Park, H.C.K., corresponding author Chang Sik Yu, Jang Hak Yoo, and Jin Cheon Kim, *Cutoff Values of Preoperative s-CEA Levels for Predicting Survivals after Curative Resection of Colorectal Cancer.* J Korean Med Sci., 2005. **20(4): 624–627**.

83. Osumi, H., et al., *Correlation between circulating tumor DNA and carcinoembryonic antigen levels in patients with metastatic colorectal cancer.* Cancer Med, 2021. **10**(24): p. 8820-8828.

84. Wang, Y., et al., *Utility of ctDNA in predicting response to neoadjuvant chemoradiotherapy and prognosis assessment in locally advanced rectal cancer: A prospective cohort study.* PLOS Medicine, 2021. **18**(8): p. e1003741.

85. Li, J.Y., et al., *Survival landscape of different tumor regression grades and pathologic complete response in rectal cancer after neoadjuvant therapy based on reconstructed individual patient data.* BMC Cancer, 2021. **21**(1): p. 1214.

86. Kotani, D., et al., *Molecular residual disease and efficacy of adjuvant chemotherapy in patients with colorectal cancer.* Nat Med, 2023. **29**(1): p. 127-134.

87. Marnell, C.S., A. Bick, and P. Natarajan, *Clonal hematopoiesis of indeterminate potential (CHIP): Linking somatic mutations, hematopoiesis, chronic inflammation and cardiovascular disease.* J Mol Cell Cardiol, 2021. **161**: p. 98-105.

88. Norcic, G., *Liquid Biopsy in Colorectal Cancer-Current Status and Potential Clinical Applications.* Micromachines (Basel), 2018. **9**(6).

Appendix

I List of abbreviations

APC	Adenomatous polyposis coli
BEAMing	Beads, Emulsion, Amplification and Magnetics
Bp	Basepairs
CEA	Carcinoembryonic antigen
cfDNA	Cell-free DNA
CHIP	Clonal hematopoiesis of indeterminate potential
CI	Confidence interval
COSMIC	Catalogue of Somatic Mutations in Cancer
CR	Complete remission
CRC	Colorectal cancer
CT	Computer tomography
CTC	Circulating tumor cells
ctDNA	Cell-free tumor DNA (oder circulating…?)
ddPCR	Dropplet digital PCR
DFS	Disease free survival
DNA	Desoxynucleotide acid
dPCR	Digital PCR
ECLIA	ElectroChemiLuminescence-ImmunoAssay
EGFR	Epithelial growth factor receptor (?)
EMT	Epithelial to mesenchymal transition
EVs	Extracellular vesicels
GAPDH	Glycerinaldehyd-3-phosphat-Dehydrogenase
gDNA	Genomic DNA
IWWD	International Watch and Wait Database
LBx	Liquid biopsy

LoD	Limit of detection
MRD	Minimal residual disease
MRI	Magnetic resonance imaging
MSI	Microsatellite instability
ncRNA	Non-coding RNA
nCRT	Neoadjuvant chemoradiotherapy
NGS	Next generation sequencing
NIPT	non-invasive prenatal testing
NSCLC	Non-small cellular lung cancer
PCR	Polymerase chain reaction
pCR	Pathological complete remission
qPCR	Quantitative PCR
RC	Rectal cancer
RNA	Ribonucleotide acid
RT	Room temperature
RT-PCR	Real-time PCR
SR	Subtotal remission
TME	total mesorectal excision
TNM	Tumor, Nodus, Metastasis (?)
TNT	Total neoadjuvant therapy
TNT	Total neoadjuvant therapy
UMI	Unique molecular identifiers
VAF	Varian allele frequency
W&W	Watch and Wait
wtDNA	Wildtype DNA

II List of figures

III List of tables

IV Acknowledgements

Zunächst möchte ich mich bei allen teilnehmenden Abteilungen bedanken: dem Institut für Pathologie und molekulare Diagnostik unter der Leitung von Herrn Prof. Dr. Bruno Märkl, der II. medizinische Klinik geleitet von Herrn Prof. Dr. Martin Trepel, der Klinik für Allgemein-, Viszeral- und Transplantationschirurgie unter der Leitung von Herrn. Prof. Dr. Matthias Anthuber, der Klinik für diagnostische und interventionelle Radiologie unter Herrn. Prof. Dr. Thomas Krönke und der Klinik für Strahlentherapie geleitet von Herrn Univ.-Prof. Dr. Georg Stüben. Diese interdisziplinäre Studie wäre ohne die reibungslose Zusammenarbeit dieser Abteilungen nicht möglich gewesen.

Allen Voran gilt mein besonderer Dank dir, Rainer, dass du mir die Möglichkeit gegeben hast, an diesem spannenden Thema zu forschen. Du hast mich in die Welt der molekularen Onkologie eingeführt und meine Leidenschaft dafür entfacht. Vielen Dank, dass ich schon so viele Jahre Teil deines Teams sein darf sowie täglich die Möglichkeit bekomme, an interessanten Projekten zu arbeiten und mein Wissen zu erweitern.

Zudem geht ein außerordentlicher Dank an die Abteilung für molekulare Pathologie, in deren Labore ich diese Forschungsarbeit durchführen durfte. Insbesondere an Dr. Sebastian Dintner, der mir stets im Labor mit Rat und Tat zur Seite stand. Außerdem möchte ich mich herzlich bei den Labormädels, Maria, Carola, Barbara, Juliane und Nadine, bedanken. Sie haben alle dazu beigetragen, dass ich mich jederzeit wohl und willkommen gefühlt habe. Ohne sie wäre ich nicht nur im Labor, sondern auch persönlich mehrmals an meine Grenzen gestoßen.

Für die überaus enge Zusammenarbeit gilt mein Dank Dr. Michael Höck. Nur durch sein Engagement konnte die Koordination dieser Studie gelingen. Einen besseren Kollegen hätte ich mir nicht vorstellen können.

Des Weiteren bin ich dankbar für die Aufnahme in das Promotionsprogramms des Universitätsklinikums Augsburg und für die Möglichkeit, hier promovieren zu dürfen.

Vielen Dank auch an meine Freundinnen, die sich zum Teil schon seit Jahrzehnten meine Sorgen sowie Probleme geduldig anhören. Ihr habt immer an mich geglaubt, seid meine größten Cheerleader und habt mich fleißig mit Drinks oder Wellness-Ausflüge abgelenkt.

Ich danke ebenso meinen Eltern Alicia und Guillermo. Ma, pa, gracias por vuestra paciencia, apoyo y la posibilidad de vivir en Alemania. Der größte Dank gilt meinem Ehemann, besten Freund, partner in crime und weltbestem Papa Michael für seine uneingeschränkte Unterstützung, Engelsgeduld und bedingungslose Liebe in jeder Lebenslage. Dank dir trage ich sowieso schon den wertvollsten Titel – „Mama“.

V Congress participations

2019	Wissenschaftstag Universitätsklinikum Augsburg
	136. Kongress der Deutschen Gesellschaft für Chirurgie
2017	Wissenschaftstag Universitätsklinikum Augsburg